The authors would like to thank the reviewers for their extensive comments on the manuscript. We have endeavoured to address all concerns. A detailed response to each of the reviewer comments follows.

Response to Reviewer 1:

The authors would like to thank the reviewer for further considering the paper. We would like to thank the reviewer for the thorough assessment of the paper and detailed notes.

Reviewer 1 wrote:

“The authors of "Greenhouse gas network design using backward Lagrangian particle dispersion modelling – Part 2: Sensitivity analyses and South African test case" have made some significant corrections to account for the reviews of their first manuscript. Regarding this, we can note the inclusion of the aggregation errors in the experiments and some critical change of point of view when analysing the results, and a better introduction to the sensitivity tests. However, there is still some critical improvement needed.
From my point of view, this text is not suitable for a second submission (see below) even though the main comment from my first review pointed out its low quality. Other comments seem to have been skipped by the authors as illustrated by their slightly selective way of answering to the reviews (see below).
Acknowledging the efforts made by the authors for revising the study (conducting new experiments), my recommendation is thus to conduct a major revision but to be aware that without a serious improvement of the text, it should be rejected once again.”

Response: We thank the reviewer for acknowledging the progression of the paper. In the third iteration of the paper we have endeavoured to remove all irritating or incoherent word usage, to ensure that the important network design results we observed are clearly communicated.

The following points were identified by Reviewer 1 and have been addressed in the updated manuscript:

Reviewer 1 wrote:

“1) Regarding the quality of the text, I now list some examples that illustrate my general feeling even though, again, it is impossible to give an exhaustive list of the problematic sentences or paragraphs:

- Some sentences which should not have survived serious proofreading: "The carbon assessment product produced monthly outputs for all the products. These products..." (l. 305); "By basing the metric to be optimised during the optimisation procedure on the result of the posterior covariance matrix of the fluxes under a given network, this score can be optimised so that the uncertainty in the estimated fluxes is reduced." (l77-79); "without the need to [...] make unnecessary assumptions

about the measurements" (l149-150)
Examples of sentences that do not work for a given page (page 3): l56, l61-63, l68-69, l77-79, l89-91”

Response: The redundancies in these lines have been corrected. The sentences have either been re-written, or entirely removed if found to be unnecessary. Similar cases were identified in the paper and corrected.

e.g **“...A reduction in the uncertainty of the estimated fluxes is only one of many considerations when determining the location of new measurement sites, but an optimal network design with this goal will provide a guide which can be included in the assessment of these new locations....”**

Reviewer 1 wrote:

“- the confusion regarding the terminology for covariance matrices was highlighted by both reviewers during the first review and the authors tried to account for this. However, it still does not work despite the explicit correction given by the second reviewer. The covariance matrices and correlations relate to errors in the fluxes, not to the fluxes themselves. Mathematically, the covariance of the estimate of the actual flux knowing the prior/posterior flux is equivalent to the covariance of the error in the prior/posterior estimate. However, in order to avoid any ambiguity about the meaning of "fluxes" in "flux covariance matrix", one should use the usual notation "error covariance matrix". This sounds like surprising to see that this mistake has been amplified in the second version of the manuscript while the same mistake for the observation error covariance has been corrected adequately.”

Response: The convention of “flux error covariance matrix” was adopted and replaced instances where “flux covariance matrix” was used.

Reviewer 1 wrote:

“Other examples of what sounds like mistakes related to basic principles of inverse modelling (but that I interpret as approximative writing and weak proofreading): l357 the justification for assuming that the authors know perfectly the ocean fluxes is that the target quantity are land fluxes;”

Response:

We can divide the ocean contribution to a given measurement into a “near field” component (within our domain) and a “far field” contribution from the rest of the global ocean. The far field contribution is covered by the influence of the boundaries. We ignore the near field contribution in our standard case, noting that the uncertainty in flux density from the ocean is an order of magnitude smaller than that from the land. We assess the significance of this omission later finding that it is, indeed, negligible. We have included more justification in the text.

“...We are not seriously assuming that we know the ocean fluxes perfectly, but for the purposes of this optimal network design, we would prefer if the terrestrial measurements focused on solving for the terrestrial fluxes. Of course, to run a full inversion, knowledge is needed about the ocean fluxes and this would be obtained through ocean based measurements. The contributions from

the ocean can be divided into the 'near-field' and 'far-field'. The far-field contributions are contained within the boundary contributions. The near-field contributions are those within our domain. A sensitivity test was conducted whereby 10% of the maximum land NEP standard deviation was allocated to the ocean grid cells..."

"the "can be" at line 257;"

Response: The phrase "can be" was replaced with "**needs to be**"

"l127: initial condition in the domain would be ok, but not "at the site" ;"

Response: This has been corrected. Here we are referring to the initial CO_2 concentration condition of the domain.

"l128-129: I do not see why the observations would easily constrain the 3D initial condition but this relate to the issue at line 127."

Response:

Peylin et al. (2005) showed that the initial condition for their European domain had an impact for about the first 5 days of their inversion period. This is roughly what one would expect from a nominal wind speed of 5m/s and a domain of order 2000km. The smaller South African domain will feel the effect for a shorter time. Real inversions are likely to be run for several months at a time or longer. Only the first week of this period would hence feel any effect of the initial condition, so it is reasonable to ignore it here. We have added text explaining this.

"...The observed concentration (c) at a measurement station at a given time can be expressed as the sum of different contributions from the surface fluxes (c_s), from the boundaries (c_b) and from the initial condition (c_i). Peylin et al. (2005) found for their European regional inversion that the initial condition had an effect on the flux estimates for only a few days. In a smaller domain, this effect will be even shorter, and therefore it is assumed that the initial condition will contribute very little to the total flux uncertainty..."

Reviewer 1 wrote:

"- the configurations and estimates discussed in paragraphs l232-l241 and l277-l286 seem to have nothing (let say nearly nothing in the case of l230-l241) to do with the configuration used in this study. However, the discussion from lines 232 to 245 looks illogical, and at least useless given the very simple set up used by the authors for the observation error in South Africa. Note the "we assumed a similar standard deviation" at line 242, while actually the authors have doubled this value."

Response: The reviewer here is referring to the discussion on how we decided upon the observation errors. We discussed different values used in the literature, as we wanted the reader to understand how the values used in our standard case and in our sensitivity test compared to the literature. In

our standard case, we used a value which fell between what Chevallier et al. (2010) (2 ppm compared to 1 ppm) and Wu et al. (2013) of 2.9 ppm used.

The real argument here concerns what should be the standard case in the paper. We believe that the simple case is the most enlightening while, when suggesting a real network, one would take account of phenomena like aggregation error. The use of an observation error covariance matrix assuming null correlations is very common in regional inversions, and particularly in network design studies, at least as a starting point. Lauvaux et al (2012a) included temporal correlations in the observation error covariance matrix as a special case, and found that it had less of an effect on the inversions solution than changing the night time observation error values. The discussion on observation error has been modified to increase its clarity.

"...Observation errors result in the values of c_{mod} differing from the observed values in c. Sources of these errors include random and systematic measurement errors, which are usually negligible at an accredited measurement station, transport model errors, and aggregation errors, which are discussed in more detail at the end of this section (Ciais et al., 2010). Baker (2000) estimated the observation error covariance matrix by comparing the monthly observation means at Mauna Loa to a smoothed line and determining the monthly standard deviations. These values ranged between 0.34 and 0.16 ppm, and so in their case a value of 1 ppm was applied for the standard deviation to each region, with the assumption that most places would have a higher standard deviation than Mauna Loa. It was also assumed that the measurement sites would be independent of one another and no temporal correlation from month to month, so the matrix was assumed to be diagonal. Wu et al. (2013) fitted the standard deviation terms of the observation error covariance matrix to available data for a mesoscale inversion study, and estimated values between 2.9 and and 3.6 ppm.

We adopted the same observation errors as for the standard case in part 1 of 2 ppm. This value falls within the range of values reported in the literature. The dominant source of observation error represented here is from the transport model. In part 1 (Ziehn et al., 2014), a sensitivity analysis was conducted by adjusting the error estimate of the observations based on the location of the station. Since there are far fewer existing stations in South Africa from which we can extract data to assess the potential transportation error, we used the same error for all stations. As part of the sensitivity analysis we assessed the impact of increasing the night time observation error uncertainty to 4 ppm to account for known errors in modelling night time atmospheric transport. In atmospheric inversions night time observations are sometimes not considered at all, achieved by drastically increasing the night time observation error uncertainties (Lauvaux et al., 2012a)..."

Reviewer 1 wrote:
"Other examples of confusing and often useless discussions: l.402-407 (hardly understandable),"

Response: This is the discussion on some of the differences between Incremental Optimisation (IO) and the Genetic Algorithm (GA), and where we introduce the GA as one of the sensitivity tests. The lines referred to above explain an essential difference – that the IO optimises by adding stations sequentially to the solution, whereas the GA starts from the first iteration with a five member solution. The five members are then modified in subsequent iterations, until a five member solution is found which meets the convergence criterion or the number of iterations is met. This explanation has been modified to improve its clarity.

"...Although IO is expected to be more computationally efficient, optimisation through a GA would also be well suited for this kind of problem, considering that this network design for South Africa is starting with so few existing stations. The GA begins with each of the solutions in the population containing five stations. Therefore all five stations are optimised simultaneously, rather than sequentially. This method therefore may be more suited to the case where there are multiple deployments, as we have. It is possible under these circumstances that the best solution for a five station network in terms of reducing the overall uncertainty for South Africa, may not include the one station which on its own reduces the uncertainty the most..."

"l300 to 311 (monthly values are converted into daily values before being converted into weekly values: why not converting monthly values into weekly values directly) ?"

Response: This explanation has been modified. The additional step of working with the daily values, a more familiar unit, was used so that we could ensure that the prior estimates were reasonable. But this step is not necessary.

"...Using this assumption, the monthly estimates for NPP were converted into weekly values, separately for day and night, to give the final uncertainty values used to construct the prior flux error covariance matrix..."

"- by regularly stating "in the Australian test case" (e.g. l.244), this study sounds like considering other cases."

Response: We have made it clear in the introduction of this paper that Part 1 is the Australian test case, and by referring to "the Australian test case" we are referring to that paper. We also stated in the introduction of the paper that we would be dealing with the South African optimal network design, and it is outlined in the objectives. We have edited the paper so that we refer to part 1 instead of "the Australian test case".

Reviewer 1 wrote:

"2) I wrote in the first review: "Additionally, the discussions regarding whether one should minimize the mean uncertainty in fluxes at pixel scale [...] rather than the uncertainty for the mean fluxes which drive to a "sensitivity test" sound absurd. These discussions and the mixing of fossil fuel fluxes and natural fluxes in the corresponding "cost functions" highlight the absence of "physical" target for the network and for this study. Consequently, the analysis of the results is rather poor."

-> these are still critical weaknesses of the paper. The introduction only states that the target = sources and sinks of CO2. However, changing the spatial resolution of the control vector and/or the metric for the optimisation procedure (i.e. the mean uncertainty at the control resolution or the uncertainty in the total fluxes over 1 month and over South Africa) changes the target of the monitoring system. Targeting the sum of anthropogenic emissions and biogenic fluxes without attempting at separating these components does not sound sensible.
On this topic, note that l206 which characterizes the control vector is critical for the paper, but that it is lost between technical details about LPDM. Equations 2 and 3 are given without any explicit

description of the vector f or of vector c (what kind of time averaging is used for the measurements ?)."

Response: The reviewer makes two points here which should be treated separately.

*1 what is the control vector for the inversion and how is it justified? Large-scale inversions have traditionally solved for regional departures from specified prior fluxes, usually ocean, terrestrial and fossil, with often some measure of land-use change or biomass burning. As we have moved to pixel-based inversions the prior flux patterns have given way to prior estimates of fluxes at each gridpoint. The control vector is usually the flux from each gridpoint or, equivalently, the departure from the prior. Separating the pixel-resolution fluxes into components is normally pointless since the Green's Function for each component flux is identical ... unless we have data like isotopes which can distinguish flux categories. It is unsurprising then that most inversions at pixel resolution treat the total flux (e.g. the long series of global studies from Chevallier and collaborators and the regional studies from Lauvaux and collaborators). Attribution of changes in the flux is possible of course but should be clearly separated from the information returned from atmospheric measurements. This point is moot when the fossil fuel flux can be considered perfectly known but this assumption (always questionable) is certainly indefensible at the resolutions we study here (Rayner et al., 2010; Asefi-Najafabady et al. 2014). We have added further explanation to the text. To ensure clarity, the vectors **f** and **c** are explicitly defined in the new manuscript.

*2 What target quantity should one optimize? This question has been discussed since the genesis of quantitative network design in this field (Rayner et al., 1996; Kaminski and Rayner, 2008). The question cannot be wished away since any real network will have multiple objectives. We believe considering more than one of these is a strength rather than a weakness of the paper.

"...The vector of the modelled concentrations c_{mod} is a result of the contribution from the sources f, described by the transport or sensitivity matrix T. The vector f can be composed of surface fluxes and boundary concentrations (Lauvaux et al., 2012a). The surface fluxes our inversion setup would solve for are the total CO_2 fluxes within a pixel, which we take to be the sum of the biospheric and fossil fuel fluxes. We aim to solve for the total flux since there is not enough information to disentangle these fluxes. In this type of inversion setup, the surface fluxes can be separated into biospheric and fossil fuel fluxes after the inversion run, using additional information regarding either the fossil fuel or biospheric fluxes (Chevallier et al., 2014)..."

"...The observed concentration (c) at a measurement station at a given time can be expressed as the sum of different contributions from the surface fluxes (c_s), from the boundaries (c_b) and from the initial condition (c_i)..."

Reviewer 1 wrote:

"3) notations in section 2.1 can be confusing (c vs cmod instead of cmeas vs c since the variable is the model c, not the vector of measured concentrations) and equation 11 is either wrong or confused by such a problem of notation (c_B is not explained, but it likely corresponds to the

boundary concentrations while the text says that it is c_b). l136: shortcut or simply an error since the uncertainty from boundaries will never be projected into the posterior uncertainty in inverted fluxes."

Response: The notation for the concentration vector has been made explicit in the new manuscript, and the vectors $\mathbf{c}_B$ and $\mathbf{c}_b$ better explained. The vector $\mathbf{c}_B$ is the concentration at the boundary, and the vector $\mathbf{c}_b$ and is the boundary's contribution to the concentration at the measurement site. The text has been corrected to reflect this. The text has also been corrected to reflect that we are considering the boundary contribution to the observation error. Since both boundary conditions and surface fluxes couple to the same observations, increases in boundary condition uncertainty will increase posterior uncertainty of fluxes. In that sense boundary condition errors do, in fact, project into posterior flux uncertainties.

"...$\mathbf{c}_{b;mod} = \mathbf{M}_B\mathbf{c}_B$
where $\mathbf{M}_B$ is the submatrix of T for the boundary concentrations, $\mathbf{c}_B$..."

Lauvaux et al (2012a), Lauvaux et al (2012b), and Peylin et al (2005) are all examples of regional inversion studies which have solved for the boundary inflow in the inversion setup. Therefore the boundary inflow has to be part of the source vector, which would required that it has associated terms in the sensitivity matrix (which we explained in section 2.7) and in the prior error covariance matrix of the sources.

Reviewer 1 wrote:

"4) the discussions about the observation errors should be rewritten. The authors seem to assume that the reader perfectly knows what observation errors correspond to (except when dealing with the aggregation errors), and that the reader is fully aware of issues with observation errors at night; however, they still give awkward details such as at line 251. Explanations regarding the aggregation errors are confusing: the part l253-275 is hardly readable unless already knowing what the author detail. For example: whose "spatial resolution" does line 254 refer to ?"

Response: The contributions to the observation error have been more clearly explained in the new manuscript, and the aggregation error further expanded. The spatial resolution refers to that of the surface fluxes, i.e. the size of the pixels. An example of the changes to the observation error section was shown in response to comment 1.

Reviewer 1 wrote:

"5) When do the authors explain that they use a regional model which is why they need boundary conditions ?"

Response: We have made this explicit in the introduction of the new manuscript, as well as explained how the GCM CCAM is run in stretched grid mode, so that acts as a regional climate

model. The GCM is zoomed in over the domain, and we use the model outputs from this region to drive the LPDM model. The processing procedure we used for the LPDM model is limited to a bounded domain (e.g. Lauvaux et al 2012a). We use a regional model, therefore requiring boundary information, since we need to resolve the atmospheric transport at a high temporal resolution, which in turn requires that the model be run at a high resolution (Sarrat et al., 2009).

"...In the case of the South African network design, these variables are produced by the CSIRO Conformal-Cubic Atmospheric Model (CCAM), a variable resolution global circulation model run in regional mode. We use the regional mode so that we can resolve the atmospheric transport at a high temporal resolution, which requires that the transport model be run at a high spatial resolution as well (Sarrat et al., 2009)..."

Reviewer 1 wrote:

"6) I still feel that this paper gives too much useless details about the system and its configuration even though there is less overlapping with the part I paper. Some examples of useless details: all the discussions about CCAM (nearly one page) ? redundancies between the beginning of section 2.2 and the end of page 6 ..."

Response: We feel that providing details on how CCAM was specified is important for this study, as the use of CCAM as a regional climate model over South Africa is still fairly novel (Engelbrecht et al, 2009). CCAM used in this study is not from the ACCESS runs, as in the case of part 1, and therefore providing details here is not redundant. The objective of this paper is to demonstrate the use of the LPDM model to produce the sensitivity matrix needed for our inversion, and providing details on the setup of CCAM gives insight into how our LPDM model is driven. The redundant detail on the setup of LPDM from part 1 has been removed.

The first sentence of the last paragraph of section 2.2 has been modified to avoid repeating information stated at the beginning of the section.

"...To determine which sources and how much of each of these sources a measurement site sees at a given moment, the sensitivity matrix T containing the influence functions is required. For a regional inversion this matrix can be directly obtained by running a Lagrangian particle dispersion model in backward mode. The particles are released from the measurement locations and travel to the surface and the boundaries (Lauvaux et al., 2008; Seibert and Frank, 2004). We used the model developed by Uliasz (1994) which we refer to as LPDM. In this mode the model simulates the release of a large number of particles from arbitrary emissions sources by tracking the motion of the particles backward in time (Uliasz, 1993, 1994). By running the model in this receptor-orientated mode the influence functions for a given receptor are calculated, as described in part 1 (Ziehn et al., 2014)..."

Reviewer 1 wrote:

"7) I do not understand the point about the aggregation error at line 304. Using values from the closest pixel in South Africa does not really sound far more sensible than a "blanket estimate" ."

Response:

One input into the calculation of aggregation error is the spatial variance of the high-resolution pixels within the low-resolution pixel. We only had access to terrestrial biosphere fluxes for South Africa. Thus, if a low-resolution pixel included points outside South Africa we needed a reasonable flux estimate. Given correlations in biome type, the nearest point in South Africa is a more reliable guide than an average. An average will also reduce aggregation error artificially since many pixels may be assigned the same value, reducing the variance.

"...As a realistic estimate, areas outside of South Africa, which had no estimates available for NPP from the carbon assessment product, were assigned the NPP estimate from the closest South Africa grid cell for a particular month. In this way, pixels to the east of the continent in the Mozambican region had similar flux uncertainties prescribed as for the northern savannah pixels within South Africa, and those on the west of the continent in Namibia had uncertainties prescribed as for the semi-desert pixels in Northern Cape Province of South Africa. This type of interpolation was carried out to avoid adding unnecessary aggregation errors at the South African terrestrial borders, which would occur if a blanket estimate for NPP outside of South Africa was used. A blanket estimate would lead to artificially large changes in the flux uncertainties between neighbouring pixels, exaggerating aggregation errors for stations near these borders, and conversely null changes in uncertainty between non-South Africa terrestrial pixels...."

Reviewer 1 wrote:

"8) around l335: rescaling uncertainties as a function of the land cover in a grid cell makes sense for the natural fluxes, but I think that it does not make sense for the anthropogenic emissions. "

Response: This sentence has been reworded to clarify our procedure. We did not multiply the fossil fuel flux errors by the fraction of land cover, only the natural fluxes.

"...The biospheric flux uncertainties were multiplied by the fraction of the grid cell covered by land, separately for day and night..."

Reviewer 1 wrote:

"9) l357-363: I do not really understand how the NEP from land ecosystems can be used to derive uncertainty in the ocean fluxes. Even if considering uncertainties in the ocean productivity only, how to relate land NEP to this ? "The nearest land NEP": the map may not look better than if a single value was used far from the coast."

Response: In the sensitivity study we considered three cases for the ocean pixel flux errors: null error; homogenous error; and inhomogeneous error. In the homogenous case, the error was assigned as 10% of the highest terrestrial NEP value. For the inhomogeneous case the NEP was also used to assign errors, but instead the closest land pixel was used. The assignment of errors for this test case was merely demonstrative, and not intended for actual use in an inversion. The purpose was to determine if inhomogeneous ocean flux errors would affect the network design differently to a homogenous assignment of errors. The question of what to assign the ocean pixels will be further

investigated in an inversion exercise using concentration measurements from a pilot study conducted over a smaller region of South Africa. We have made it clear in the new manuscript that we would not use the nearest land based pixels to determine ocean flux error estimates.

"...A sensitivity test was conducted whereby 10% of the maximum land NEP standard deviation was allocated to the ocean grid cells. This uncertainty represents the uncertainty in the ocean productivity models which would be used to obtain prior estimates of ocean fluxes during an inversion, which are similar to the values allocated by Chevallier et al. (2010). A second case was considered where 10% of the nearest land NEP uncertainty was allocated to each ocean grid cell, so that the uncertainties of the ocean grid cells would increase as the uncertainties of nearby land fluxes increased. The purpose of this test case was only to demonstrate the effect implementing a variable ocean uncertainty scheme..."

Reviewer 1 wrote:

"10) equation 7 does not really correspond to something consistent between the different experiments: when changing the resolution of the control vector, it targets a different space scale. Therefore, comparing results obtained with such a metric when using different resolutions of the control vector may not really make sense. One should rather have selected a metric that corresponds to a fixed horizontal resolution of the fluxes that could be addressed by any of the control vectors tested in this study.

Again, the discussion at lines 386-387 sounds absurd. It does not make sense to question whether it is better to be interested in improving the mean knowledge on local fluxes or on the total fluxes (which is the translation of whether it is better to use metric from eq 7 or 8). See also the major comment 2."

Response: The reviewer does not explain why the question does not make sense. It is an absolute prerequisite of sound experimental design that the target of the experiment is well understood but, as discussed above, there is rarely a single use for a trace gas network or, as with the global network, its use will evolve over time. As explained for comment 2, the sensitivity tests were setup so that they could be compared to the standard case. And in addition, the networks were compared by their percentage uncertainty reduction, rather than absolute reduction. The inclusion of equation 7 to be used in the cost function of the optimisation procedure was mainly to compare it to the standard case of using the sum of the covariance elements. We have included in our discussion that equation 8 is the preferred metric for assessing the overall uncertainty in fluxes for a domain, and used by most network design papers.

"...The use of equation 7 results in the minimisation of the average variability between surface pixels. Equation 8 is the more accepted metric to calculate uncertainty for network designs, and it results in the minimisation of the uncertainty of the total flux over South Africa. As for part 1 (Ziehn et al., 2014) and as used by Rayner et al. (1996), we use J_{Ce} as the uncertainty metric for the standard design..."

Reviewer 1 wrote:

"11) Section 2.6 starts with redundancies and ends with 2 sentences saying the same thing."

Response: This paragraph on the measurements sites has been rewritten to improve clarity.

"...Hypothetical stations were selected from a regular grid over South Africa, resulting in 36 equally spaced locations (Fig. 3), from which five stations need to be selected. Ultimately, the exact location of the stations will be determined by practical considerations, such as the presence of existing infrastructure, such as communication towers and meteorological stations, available manpower, the relative safety of the instruments, and the accessibility of the sites. The optimal network will be used as a guide as to which locations are ideal. Once station sites have been chosen, it will be possible to again calculate the posterior flux error covariance matrix based on the exact tower locations, and determine how close to the idealise uncertainty reduction the implemented network can achieve..."

Reviewer 1 wrote:

"12) End of section 3.1: the authors likely misunderstood the comment from reviewer 2 about the correlations due to errors in the boundary conditions. He questioned about correlations in the observation error due to errors in the boundary conditions which definitely increase the weight of such an error over long time periods. This could be critical when assessing the budget of fluxes in South Africa over 1 month."

Response: We do not believe we misunderstood the comment. During the first review, Reviewer 2 stated "*The other and probably more important point to note is that Equation 1 obviously uses an uncorrelated error of the concentration at the boundary. In fact, at the model resolution, one would expect high error correlations in space and time, which would magnify Cb"*. Here the reviewer is explicitly referring to the uncorrelated error of the concentration at the boundary. The equation referred to here is $c = c_s + c_b + c_i$, where c_b is the contributions from the boundary. These contributions can be modelled as $\boldsymbol{c}_{b\,mod} = \mathbf{M}_B\mathbf{c}_B$, where $\mathbf{c}_B$ represents the concentrations at the boundary. The expression $\mathbf{C}_b = \mathbf{M}_B\mathbf{C}_I\mathbf{M}_B^T$ gives the posterior covariance matrix of the boundary contributions, where $\mathbf{C}_I$ is the prior error covariance matrix of the boundary concentrations.
We wish to recover information on $\mathbf{s}$ from $\mathbf{c}$ for which $\mathbf{c}_i$ and $\mathbf{c}_b$ are sources of noise. What is important is not the correlations in $\mathbf{c}_b$ but rather the correlations they induce on $\mathbf{c}$ itself. We show that the magnitudes of $\mathbf{C}_b$ are small so that the perturbation they make to the hitherto uncorrelated uncertainty covariance for $\mathbf{C}_c$ is also small. This is why we can safely neglect $\mathbf{c}_b$ in this setup. We stress that this may not hold for a smaller domain.

Reviewer 1 wrote:

"13) I do not really see what the plot of the footprints (Figure 4) is supposed to illustrate. It sounds like the beginning of section 3.1 is redundant with the explanation about the derivation of the sensitivity matrix earlier."

Response: The purpose of this section is firstly to justify the exclusion of the boundary concentration errors from the observation error covariance. This section was presented here, since we felt it belonged more with the results section than under the methods section. It's a finding of the paper.

The footprints were included, firstly to show why it was necessary to expand the observation network, and secondly to show results of the LPDM, which to our knowledge has not been run over the domain of South Africa before. These plots also provide insight to the reader on the field of view of a selection of potential measurement sites.

"...The particle counts generated during the LPDM runs for each station were summed over the month in order to obtain a footprint of each station. To illustrate this, plots of the influence footprint in January (Fig. 4) are provided, using a logarithmic scale, for Cape Point and three other candidate stations: 28 (near Potchefstroom), 18 (near Mthatha), and 4 (near Port Elizabeth). For both January and July, the influence footprints show that the three candidate stations have more contributions from terrestrial South African sources than Cape Point has. The plots show that the majority of influence for a site is from the sources in the surrounding pixels..."

Reviewer 1 wrote:

"14) Section 4 exploits few of the details from section 3. Therefore, much of the details in section 3 seem useless while this section is relatively short. This highlight a lack of more relevant analysis."

Response: The purpose of section 3 is to give detailed discussion on the results of the network design, and the comparison between the different sensitivity tests. In section 4 we present the "take-home" messages from these discussions, and therefore do not discuss explicit results, which has already been done in section 3. We have expanded on section 3 to include information on the total flux uncertainties estimated under the base network and under the different optimal networks.

e.g. **"...The network solution for July was able to achieve a reduction in uncertainty in the total South African flux from 6.42 gC/m^2/week under the base network to 3.66 gC/m^2/week under the optimal network..."**

Reviewer 1 wrote:

"15) Given the small number of sites to be added in the network, I feel that the "DI" diagnostic is a bit artificial and useless while section 2.8 is hardly readable. Looking at the maps bring more insights about the similarity between the networks than table 4."

Response: We disagree with the reviewer on the usefulness of the Dissimilarity Index (DI). This diagnostic allows the reader to assess the difference between two network solutions in an objective manner, without having to rely on "eye-balling" the differences, which we were criticized for in the first review of the paper. We note that this diagnostic was added in response to the comments from the reviewer during the first review of the paper. The DI gives a measurement, in metres, of how different two network solutions are, which can consistently be used to compare networks, provided that all the network solutions contain the same number of members. This measure will be explicitly formulated to highlight this property.

"...A dissimilarity index (DI) was calculated as the sum of the distance to the nearest neighbour in the compared network, over all the members in the pair of assessed networks.

$$DI = \sum_{i=1}^{5} min\sqrt{\Delta x_{ij}^2 + \Delta y_{ij}^2} + \sum_{j=1}^{5} min\sqrt{\Delta x_{ij}^2 + \Delta y_{ij}^2}$$

where i and j E [1,2,3,4,5], and Δx^2_{ij} and Δy^2_{ij} are the squared differences between the Cartesian coordinates of the ith station in network 1 and the jth station in network 2. In cases where the two networks compared were the same, the index results in a value of zero. The index increases as the networks become more dissimilar in space. This provides a one-number measure of network similarity that can consistently be used for the network comparisons provided each solution consists of the same number of stations. The index provides a measure in kilometres of how

different two network solutions are. This allows for an objective assessment of how different the positioning of sites are between two network solutions which may not be obvious to the eye..."

Reviewer 1 wrote:

"16) The new discussion at lines 690-695 does not make sense to me. If the aggregation error is perfectly set-up in the inversion system, the inversion will provide the same results for large areas (here for the whole South Africa) when solving for the fluxes at coarse or high resolution. I assume that this is not the case here because the estimate of the aggregation errors has been simplified e.g. through ignoring temporal correlations in this error. L695 sounds strange."

Response: During the first review of this paper, Reviewer 1 stated "In inversion systems, computational costs prevent from working at very high resolution over the whole domain, which explains why there have been some attempts at optimizing the horizontal grid for the fluxes to be controlled as a function of the station locations. But if there was no computational or technical limitation, one should use a very high resolution over the whole domain in order to derive results as realistic as possible (bearing aggregation errors that are as small as possible)."

In lines 690 to 695 we are discussing the results of our aggregation assessment which showed that large aggregation errors are a problem for regional inversion studies. Large errors occur when the spatial resolution of the sources is low, but the spatial resolution of the transport model is high. This discussion will be modified to make this clearer. Previous regional inversion studies have also added aggregation errors to the diagonal elements of the observation error covariance matrix (e.g. Lauvaux et al 2012). Kaminski et al (2001) also state that this simple adjustment of the observation errors will assist in reducing aggregation errors in the flux estimates. But even if the aggregation errors were specified perfectly, the total flux estimate for South Africa will only be similar between the high and low resolution cases. Accounting for the aggregation errors do not exactly compensate for the loss of information due to aggregation (Wu et al. 2011).

The way we treat the fossil fuel flux uncertainty leads to the higher resolution case resulting in higher total flux uncertainty for South Africa. For the low and high resolution cases, we create the surface of flux uncertainties using the same procedure. For each of the ten realisations from the FFADS product, we regrid the 0.1°×0.1° fossil fuel emissions onto the surface grid we are using. To obtain the uncertainty estimates the within pixel variance is calculated for the ten realisations. The result of carrying this procedure out at higher spatial resolutions is that the variance values are larger compared to lower resolutions, and the between pixel variability is increased (Asefi-Najafabady et al. 2014). This results in much larger values in the prior flux error covariance matrix, which correspond to larger values in the posterior flux error covariance matrix and a larger total flux uncertainty for the domain. This in part explains why, despite accounting for aggregation, the uncertainties for the total flux for South Africa is different between the different resolutions, with the uncertainty increasing as the spatial resolution increases.

Line 695 has been modified to:
" ... The spatial resolution of the sources also determines the dimensions of the sensitivity matrix and prior flux covariance matrix, which impacts on the computational resources required to run an inversion or network optimisation...."

Reviewer 1 wrote:

“17) Similarly, the new discussion at lines 723-728 does not make sense to me neither. There is the same need for confidence on the knowledge about correlations in the prior error when using null or positive correlations (and lines 339-340 favour having positive correlations). If you use null correlation but that you actually do not have any idea about whether it is more realistic than assuming positive correlations, this yields a budget of uncertainty over South Africa which is not reliable and thus the network optimization procedure can be driven by a wrong diagnostic. Therefore, I do not understand why using null correlations is presented as a safety measure. In principle, the stronger constraint when using correlations has no reason to be problematic. Checking the realism of the budgets of prior and posterior uncertainties when aggregating over South Africa would have helped raise insights on the set up of the correlation in this study. But such numbers are never analysed or discussed in this paper. The last sections focus on scores of uncertainty reduction only.”

Response:

First we note the relatively weak error correlations found by Chevallier et al (2010) especially when considering pixels with different ecosystem types. Thus it is probably less important than one might expect to specify the structure of these correlations correctly. Secondly, the choice of independent priors is conservative since background covariances tend to spread the influence of observations further, thus enhancing the constraint of a given network. The correlation structure is model-dependent and thus hard to specify without repeating the work of Chevallier et al. (2010) for each biosphere model. For these reasons it seems prudent to treat the control case as independent and consider a correlated case for a sensitivity study.

In answer to the reviewer's final point, when considering the relative performance of different networks (the purpose of this study) absolute and relative error reductions are equivalent.

“...For a network to be based on a prior covariance matrix including correlation, there would need to be confidence that this correlation structure and size of correlations between fluxes were accurate. This is generally not the case, and easier to assess when concentration measurements are available, which is why many network designs have assumed independence between prior fluxes (Rayner, 2004; Patra and Maksyutov, 2002). Including correlations which are too large can lead to an over constrained system (Lauvaux et al., 2012), which is evidenced in this study where the uncertainty reductions were the largest under the correlation test case..."

Response to Reviewer 3:

Reviewer 3 wrote:

“Review of the paper entitled: Greenhouse gas network design using backward Lagrangian particle dispersion modeling – Part 2: Sensitivity analyses and South African test case” by Nickless et al.

The paper presents the results from a network design study for a CO2 flux inversion over South Africa. It is clearly written and the scientific results are highly relevant to network design study in general. The main weakness is that new ideas are not clearly stated in the abstract. Some aspects of this work were never presented before to the best of my knowledge (e.g. compare 3 different methods to select the network, sensitivity tests to boundary concentrations, …). This paper should be considered for publication after considering the minor revisions listed hereafter.”

Response: The authors would like to thank the reviewer for the favourable review and for pointing out which aspects of our research we have not fully highlighted.

Reviewer 3 wrote:

“Technical comments:

Boundary influence: The influence from outside the modeled domain is presented similarly to the surface flux, i.e. additional unknowns in the state vector. When you consider that the boundary concentration uncertainty should be smaller than the observation errors, the problem of potential biases in the concentrations, which could affect all the towers at once, is ignored. Actually, the inversion system is not really built to optimize the boundary concentrations but instead the surface fluxes. The idea is to provide the best information possible for the boundary concentrations. This could mean that some sites would be used to constrain the boundary concentrations. In this case, the error reduction of the boundary concentrations is secondary, and you would focus on dedicating sites able to measure the boundary inflow, i.e. minimize the sensitivity to the surface fluxes and maximize the error reduction of the boundary concentrations.”

Response: For the inversion setup that we use in this paper, similar to that of Lauvaux et al (2012a), we consider solving for the boundary contributions (or the boundary inflow) as an explicit source. This is made possible through the use of the particle counts from the backward LPDM model which we use to determine the sensitivity of each measurement site to the concentrations at the boundary. Therefore the sensitivity matrix would then contain extra columns for each of the boundaries for each week (if we’re considering contributions from a weekly averaged concentration at the boundary). Having measurement stations specifically for measuring boundary inflow would be useful, but would then reduce the number of station we have left to resolve the surface fluxes, which we are specifically aiming at in this study. We deliberately chose a large domain with South Africa situated in the middle so that the boundary contributions would be minimal. See response to Reviewer 1 comment 3.

Reviewer 3 wrote:

“L28: The statement is correct but very abrupt for an introduction. Please rephrase the sentence, starting from the beginning of the scientific problem, which may be your second sentence actually.”

Response: The beginning of the introduction has been amended to introduce the issue of climate change, and why CO_2 sources need to be monitored and better modelled.

“...Mitigating climate change is one of the great challenges of our time. To further this end, it has become essential to accurately estimate the emission and uptake of CO2 around the globe...”

Reviewer 3 wrote:

“L103: “LPDM” is also a very common acronym for any LPD model. Use the original reference with the acronym to clarify.”

Response: We have clarified this in the text.

“...For a regional inversion this matrix can be directly obtained by running a Lagrangian particle dispersion model in backward mode. The particles are released from the measurement locations and travel to the surface and the boundaries (Lauvaux et al., 2008; Seibert and Frank, 2004). We used the model developed by Uliasz (1994) which we refer to as LPDM...”

Reviewer 3 wrote:

“L160: “…driven by three-dimensional fields…” but you indicate only (u,v).”

Response: This has been corrected to **“(u,v,w)”**.

Reviewer 3 wrote:

“Observation error covariance matrix: The errors are defined using reasonable estimates from the literature, corrected with your own aggregation error estimates. The only aspect of the problem that would be worth considering here is the local atmospheric dynamics that could affect specific locations. Considering the spatial resolution used for CCAM, and prior knowledge about site locations such as topography, the distance to the coastline, … Would site 12 be correctly simulated by CCAM for example?”

Response: At this stage CCAM has not been sufficiently tested against measured data to determine the degree of transport errors at different locations in South Africa. But this analysis will be performed for a pilot inverse modelling exercise around a South African city, where three measurement stations will be used to assess how well CCAM is able to model atmospheric transport over fairly complex terrain.

Reviewer 3 wrote:

“L351: do you really mean that you multiplied the correlation coefficients? This approach reduces the correlation rapidly in space and time. In the example (0.3 x 0.5), the correlation is almost negligible (i.e. 0.15).”

Response: Yes, in the sensitivity test we used a fairly simple correlation structure with a short correlation length. Wu et al (2013) found that spatial correlations with long correlation lengths were not supported in their mesoscale inversion and Chevallier et al. (2010) found short correlation lengths in their analysis of biosphere models.

Reviewer 3 wrote:

“L386-387: It is unclear why you wouldn’t use the total uncertainty. The theory would suggest that you use Jce and consider all the elements of the posterior covariance matrix. Do you mean that, because non-diagonal elements are less certain, you may not want to consider them in your optimization?”

Response: We agree with the reviewer that the total uncertainty is the better metric. The trace was only included because it is a possible alternative. The emphasis on the preference for the use of the total uncertainty metric is stated in the updated manuscript.

“...The use of equation 7 results in the minimisation of the average variability between surface pixels. Equation 8 is the more accepted metric to calculate uncertainty for network designs, and it results in the minimisation of the uncertainty of the total flux over South Africa...”

Reviewer 3 wrote:

“L524: “0.0 ppm” sounds very low (as close as it can be from being negative in fact). Was it that low or is it just a typo?”

Response: The concentrations have been rounded to two significant digits to show that the smallest aggregation error was determined to be 0.01 ppm.

Reviewer 3 wrote:

“L534: “spin up” refers to the time window used to count particles backward in time? How was it defined in your simulations? Would an observation on the second day of the month have only two days of backward transport?”

Response: During the assessment of the aggregation error, we realised that the first week’s transport was not well represented by the LPDM model. Yes, day one would only have had one day of transport. Therefore we based all our calculations on the last two weeks of the month. This is emphasized in the updated version of the manuscript. The statement on “spin up” was explaining that when using the LPDM model, it is a better to run the model with at least a week, if not perhaps

an additional month's worth of forcing data at the beginning of the time domain, so that the transport is accurate over the period of interest.

"...When running LPDM to generate the sensitivity matrix, it is imperative to specify a sufficient number of particles per release, as well as to run the model for longer than required, with additional time at the beginning of the run. This is to avoid transport errors, and to avoid exaggerating the aggregations errors..."

Reviewer 3 wrote:

"L610: Looking at Figure 7, the sensitivity tests for January are converging on four sites, even though none of them includes all the cases, and 6-7 other sites. This is fairly similar to the convergence of July, slightly weaker maybe, but well defined too."

Response: Similar convergence definitely does appear to be taking place in January as well. The most convergence appears to take place in the combine January/July run, with four very clear sites. This is highlighted in the updated manuscript.

"...Similarly to July, the network solutions do appear to converge towards three stations, but different from those in July..."

References

Asefi-Najafabady, S., Rayner, P. J., Gurney. K. R., McRobert, A., Song, ., Coltin K., Huang, J., Elvidge, C., and Baugh, K.: A multiyear, global gridded fossil fuel CO2 emission data product: Evaluation and analysis of results, J. Geophys. Res., 119, doi: 10.1002/2013JD021296, 2014

Chevallier, F.,Wang, T., Ciais, P., Maignan, F., Bocquet, M., Arain, M. A., Cescatti, A., Chen, J., Dolman, A. J., Law, B. E., Margolis, H. A., Montagnani, L., and Moors, E. J.: What eddy-covariance measurements tell us about prior land flux errors in CO2-flux inversion schemes, Global Biogeochem. Cy., 26, GB1021, doi: 10.1029/2010GB003974, 2012.

Chevallier, F., Palmer, P. I., Feng, L., Boesch, H., O'Dell, W., and Bousquet, P.: Toward robust and consistent regional CO2 flux estimates from in situ and spaceborne measurements of atmospheric CO2, Geophys. Res. Lett., 41, 1065–1070, doi:10.1002/2013GL058772, 2014.

Engelbrecht, F. A., McGregor, J. L. and Engelbrecht, C. J.: Dynamics of the conformal-cubic atmospheric model projected climate-change signal over southern Africa, Int. J. Climatol., 29, 1013-1033., doi: 10/1002/joc.1742.29., 2009.

Kaminski, T., Rayner, P .J., Heimann, M., and Enting, I. G.: On aggregation errors in atmospheric transport inversions, J. Geophys. Res., 106, 4705–4715, 2001.

Kaminski, T., Rayner, P .J.: Assimilation and Network Design, In: The Continental-Scale Greenhouse Gas Balance of Europe, Ecological Studies Volume 203, pp. 33-52, doi: 10.1007/978-0-387-76570-9_3, 2008.

Lauvaux, T., Uliasz, M., Sarrat, C., Chevallier, F., Bousquet, P., Lac, C., Davis, K. J., Ciais, P., Denning, A. S., and Rayner, P. J.: Mesoscale inversion: first results from the CERES campaign with synthetic data, Atmos. Chem. Phys., 8, 3459–3471, doi: 10.5194/acp-8-3459-2008, 2008.

Lauvaux, T., Schuh, A. E., Uliasz, M., Richardson, S., Miles, N., Andrews, A. E., Sweeney, C., Diaz, L. I., Martins, D., Shepson, P. B., and Davis, K. J.: Constraining the CO2 budget of the corn belt: exploring uncertainties from the assumptions in a mesoscale inverse system, Atmos. Chem. Phys., 12, 337–354, doi: 10.5194/acp-12-337-2012, 2012a.

Lauvaux, T., Schuh, A. E., Bouquet, M., Wu, L., Richardson, S., Miles, N., and Davis, K. J.: Network design for mesoscale inversions of CO2 sources and sinks, Tellus, 64B, doi:10.3402/tellusb.v64i0.17980, 2012b.

Peylin, P., Rayner, P. J., Bousquet, P., Carouge, C., Hourdin, F., Heinrich, P., Ciais, P., and AEROCARB contributors: Daily CO2 flux estimates over Europe from continuous atmospheric measurements: 1, inverse methodology, Atmos. Chem. Phys., 5, 3173–3186, doi:10.5194/acp-5-3173-2005, 2005.

Rayner, P. J., Enting, I. G., and Trudinger, C. M.: Optimizing the CO2 observing network for constraining sources and sinks, Tellus B, 48, 433–444, 1996.

Rayner, P. J., Raupach, M. R., Paget, M., Peylin, P., and Koffi, E.: A new global gridded data set of CO2 emissions from fossil fuel combustion: mehodology and evaluation, J. Geophys. Res., 115, D19306, doi: 10.1029/2009JD013439, 2010.

Sarrat, C., Noilhan, J., Lacarr`ere, P., Ceschia, E., Ciais, P., Dolmon, A. J., Elbers, E. J., Gerbig, C., Gioli, B., Lauvaux, T., Miglietta, F., Neininger, B., Ramonet, M., Vellinga, O., and Bonnefond, J. M.: Mesoscale modelling of the CO2 interactions between the surface and the atmosphere applied to the April 2007 CERES field experiment, Biogeosciences, 6, 633–646, doi:10.5194/bg-6-633-2009, 2009.

Seibert, P. and Frank, A.: Source-receptor matrix calculation with a Lagrangian particle dispersion model in backward mode, Atmos. Chem. Phys., 4, 51–63, doi: 10.5194/acp-4-51-2004, 2004.

Uliasz, M.: The atmospheric mesoscale dispersion modeling system, J. Appl. Meteorol., 31, 139–149, 1993.

Uliasz, M.: Lagrangian particle modeling in mesoscale applications, in: Environmental Modelling II, Computational Mechanics Publications, Southampton, UK, 71–102, 1994.

Wu, L., Bocquet, M., Lauvaux, T., Chevallier, F., Rayner, P. J. and Davis, K.: Optimal representation of source-sink fluxes for mesoscale carbon dioxide inversion with synthetic data, J. Geophys. Res., 116, D21304, doi:10.1029/2011JD016198, 2011.

Wu, L., Bocquet, M., Chevallier, F., Lauvaux, T., and Davis, K.: Hyperparameter estimation for uncertainty quantification in mesoscale carbon dioxide inversions, Tellus B, 65, 20894, doi: 10.3402/tellusb. v65i0.20894, 2013.

Ziehn, T., Nickless, A., Rayner, P. J., Law, R. M., Roff, G., and Fraser, P.: Greenhouse gas network design using backward Lagrangian particle dispersion modelling - Part 1: Methodology and Australian test case, Atmos. Phys. Chem., 14, 9363-9378, 2014.

Manuscript prepared for Atmos. Chem. Phys.
with version 5.0 of the LaTeX class copernicus.cls.
Date: 25 January 2015

Greenhouse gas network design using backward Lagrangian particle dispersion modelling - Part 2: Sensitivity analyses and South African test case

A. Nickless[1,2], T. Ziehn[3], P.J. Rayner[4], R.J. Scholes[1], and F. Engelbrecht[5]

[1]Global Change and Ecosystem Dynamics, CSIR, Pretoria, 0005, South Africa.
[2]Department of Statistical Sciences, University of Cape Town, Cape Town, 7701, South Africa.
[3]Centre for Australian Weather and Climate Research, CSIRO Marine and Atmospheric Research, Aspendale, VIC 3195, Australia.
[4]School of Earth Sciences, University of Melbourne, Melbourne, VIC 3010, Australia.
[5]Climate Studies and Modelling and Environmental Health, CSIR, Pretoria, 0005, South Africa.

Correspondence to: Alecia Nickless
(ANickless@csir.co.za)

Abstract. This is the second part of a two-part paper considering a measurement network design based on a Lagrangian stochastic particle dispersion model~~(LPDM), aimed at performing a sensitivity analysis~~, which we referred to as LPDM, in this case for South Africa. A sensitivity analysis was performed for different specifications ~~in a network design applied to a~~ of the network design parameters which were applied to this South African test case. ~~The~~ LPDM, which can be used to derive the sensitivity matrix used in an atmospheric inversion, was run for each candidate station for the months of July (representative of the Southern Hemisphere Winter) and January (Summer). The network optimisation procedure was carried out ~~for South Africa~~ under a standard set of conditions, similar to those applied to the Australian test case in part 1, for both months and for the combined two months, using the Incremental Optimisation (IO) routine. The optimal network design setup was subtly changed, one parameter at a time, and the optimisation routine re-run under each set of modified conditions, and compared to the original optimal network design. The assessment of the similarity between network solutions showed that changing the height of the surface grid cells, including an uncertainty estimate for the ocean fluxes, or increasing the night time observation error uncertainty did not result in any significant changes in the positioning of the stations relative to the standard design. However, changing the covariance matrix or increasing the spatial resolution did.

Large aggregation errors were calculated for a number of candidate measurement sites using the resolution of the standard network design. Spatial resolution of the prior fluxes should be kept as close to the resolution of the transport model as the computing system can manage, to mitigate the exclusion of sites which could potentially be beneficial to the network. Including a generic

correlation structure in the prior flux covariance matrix lead to pronounced changes in the network solution. The genetic algorithm (GA) was able to find a marginally better solution than the IO procedure, increasing uncertainty reduction by 0.3%, but still included the most influential stations from the standard network design. In addition, the computational cost of the GA compared to IO was much higher. Overall the results suggest that a good improvement in knowledge of South African fluxes is available from a feasible atmospheric network and that the general features of this network are invariable under several reasonable choices in a network design study.

1 Introduction

~~It~~ Mitigating climate change is one of the great challenges of our time. To further this end, it has become essential to accurately estimate the emission and uptake of CO_2 around the globe. Greenhouse gases affect the absorption, scattering and emission of radiation within the atmosphere and at the Earth's surface (Enting, 2002; Denman et al., 2007). Of these gases, CO_2 contributes the greatest forcing on the climate (Canadell et al., 2007). Monitoring CO_2 sources and sinks is necessary for validating important components of climate models and for determining the best course of action to mitigate Climate Change. The method of inverse modelling can be used to estimate the magnitude of sources and sinks of CO_2 at different temporal and spatial scales (Enting and Mansbridge, 1989; Rayner et al., 1999; Rödenbeck et al., 2003; Chevallier et al., 2010). This method relies on precision measurements of atmospheric CO_2 concentrations to refine the prior estimates of the CO_2 fluxes. Using the machinery of atmospheric inversion, an optimal network of new sites to add to the existing infrastructure for measurement of atmospheric CO_2 concentrations can be derived from a list of potential sites.

Previous optimal network studies run at the global scale have highlighted southern Africa as a region ~~of~~ associated with large uncertainty in its terrestrial CO_2 fluxes, requiring further constraint by measurements (Patra and Maksyutov, 2002). Measurements over Africa are much sparser compared to other continents. Only the Cape Point Global Atmospheric Watch (GAW) station has a long term CO_2 concentration record, measuring since 1992. This tower was located at Cape Point (34.35° S, 18.49° E) predominantly to record baseline measurements of well-mixed, clean air originating over the Southern Ocean. A study by Whittlestone et al. (2009) demonstrated that it would be difficult to improve estimates of terrestrial CO_2 fluxes for southern Africa using the Cape Point station alone. In 2012, an atmospheric observatory was installed near the Gobabeb Training and Research Centre, on the west coast of Namibia (22.55° S, 15.03° E), which continuously measures trace gases, including CO_2 (Morgan et al., 2012). To build on this rudimentary network, and to improve estimates of CO_2 fluxes at least for South Africa, high precision instruments for measuring atmospheric CO_2 concentrations have been purchased, ~~and~~ which are to be installed at sites, yet to be determined, across South Africa. To maximise the impact of these stations on the estimation of CO_2 fluxes

across South Africa, an optimal network design can be used to indicate the best placement of new stations with the aim of reducing the uncertainty of the terrestrial CO_2 source and sink estimates. ~~The uncertainty in the~~ A reduction in the uncertainty of the estimated fluxes is only one of many considerations when determining the location of new measurement sites, but an optimal network design ~~based on uncertainty reduction~~ with this goal will provide a guide which can be included in the assessment of these new locations. Part 1 of this paper conducted ~~a similar~~ an optimal network design study for Australia~~on how to augment~~ , hereafter referred to as part 1, aimed at augmenting its current observation network, and introduced the methodology employed in this study (Ziehn et al., 2014).

An optimal network design ~~has two basic requirements: an inversion algorithm, which is used to calculate the quantity which is to be optimised and which will be dependent on the subset of measurement sites considered, and an optimisation procedure, for selecting between possible elements in the network~~ requires the theory of atmospheric inversions to generate the posterior error covariance matrix of the CO_2 fluxes which would be estimated from a given network of stations. From this the reduction in uncertainty can be determined. The second requirement is an optimisation routine which will select between a list of potential sites (Rayner et al., 1996; Patra and Maksyutov, 2002; Rayner, 2004). Part 1 of this paper sought to reduce the uncertainty of Australian terrestrial fluxes by 50 %, and began by considering the addition of new stations to the existing base network (Ziehn et al., 2014). Similarly, the Cape Point and Gobabeb stations make up a base network of CO_2 monitoring stations for southern Africa~~, and this~~ . This optimal network design will ~~provide a theoretical study on the optimal locations of new stations within South Africa. The optimal network will add five~~ add five new measurement stations to our base network to best reduce the uncertainty in flux estimates across the country, and under the assumption of continuous, hourly measurements of CO_2 concentrations.

The ~~uncertainty metric used in the optimisation procedure is based on the posterior covariance matrix of the fluxes, estimated through the inversion procedure, which we use to represent the uncertainty in the estimated fluxes. The calculation of the posterior flux covariance matrix~~ posterior flux error covariance matrix used to derive the uncertainty metric does not require any knowledge of the measured concentrations or of the prior fluxes, only of the prior error covariance matrix of the fluxes, the error covariance matrix of the observations, and the sensitivity matrix, which are all determined separately. ~~By basing the metric to be optimised during~~ Basing the cost function of the optimisation procedure on the result of the posterior error covariance matrix of the fluxes under a given network ~~, this score can be optimised so that~~ ensures the uncertainty in the estimated fluxes under the final network solution is reduced. As ~~for the Australian test case~~ in part 1 (Ziehn et al., 2014), the incremental optimisation (IO) procedure was used for the standard optimal network design in this study. We used a regular grid of potential stations for the South African case study. The reason for doing is that, unlike Australia, South Africa does not have the relatively dense network

of meteorological stations suitable for atmospheric monitoring. Therefore, if we were to base the network on the existing sparse network of stations, we could exclude important sites which may provide better constraint. Therefore we have chosen the regular grid, and the sites selected in the optimal network can then be further investigated to determine if there is infrastructure available, such as meteorological stations, communication towers or other research facilities, which could be amenable to atmospheric measurements.

~~In addition to providing an~~ As well as providing this first-time optimal network design ~~for~~ focusing on CO_2 flux estimation over South Africa, ~~this paper aims to assess the sensitivity of the network design to a number of the parameters and choices which were necessary to run an optimal network design as proposed in this study~~the paper presents a sensitivity analysis of several parameters needed in the optimisation routine. For the standard case we used parametrisations which were most commonly implemented in the literature. We then considered alternatives and determined their impact on the network. This ~~type of~~ analysis is important because as shown by Rayner et al. (1996), certain changes to the optimisation problem, such as changing the quantity to be optimised even if very similar in nature to the original, can result in drastically different placement of stations. This would ultimately impact on the implemented network design used in deployment of the new stations. By having alternative network solutions based on parametrisation changes, we can assess how important certain stations are, since these should remain constant ~~despite parameter~~ from one network solution to the next despite these changes, and it provides insight into ~~parameter specifications which will~~ which parameters are likely to be important for the estimation of fluxes using the new network of measurement sites.

The inversion procedure requires a sensitivity matrix which calculates the contribution of the different sources to the CO_2 concentration at a particular measurement site. We used the Lagrangian ~~Particle Dispersion Model (LPDM)~~ stochastic particle dispersion model which we refer to as LPDM, driven by the global circulation model CCAM run in stretched grid regional mode, to determine this matrix. One set of parameters that we considered for the sensitivity analyses related to the specified dimensions of the surface grid box in which the particles provided by LPDM are counted. This ~~determines~~ is determined by the spatial resolution of the problem. The next set of parameters we considered relates to the two error covariance matrices which are needed for the calculation of the posterior flux error covariance matrix. We changed how these matrices were parametrised and assessed the consequences for the optimal network design. Finally we implemented an alternative optimisation procedure to IO and considered the optimisation of a different metric of uncertainty in the fluxes. As the alternative optimisation procedure, we used the genetic algorithm (GA), as described by Rayner (2004), which uses a very different optimisation philosophy to the IO method.

This paper proceeds by introducing the inversion methodology, followed by an explanation of the different sensitivity tests. The results are then presented for the South African optimal network design under the standard conditions, followed by a comparison of the sensitivity tests. The conclu-

sions provide insight into the most influential locations identified, and discuss courses of action to address the optimal network design parameters highlighted in the study.

2 Methods and the South African Test Case

2.1 Surface Flux Inversion

The Bayesian synthesis inversion method, first proposed by Tarantola (1987) and used for the network design in this paper, is the most common method used for solving atmospheric inverse problems in the literature (Rayner et al., 1996; Bousquet et al., 1999; Kaminski et al., 1999; Rayner et al., 1999; Gurney et al., 2002; Peylin et al., 2002; Gurney et al., 2003; Law et al., 2003; Baker et al., 2006; Ciais et al., 2010; Enting, 2002). The ~~inversion method~~ regional inversion method we implemented is explained in detail in part 1 (Ziehn et al., 2014). The observed concentration (c) at a measurement station at a given time can be expressed as the sum of different contributions from the surface fluxes (c_s), from the boundaries (c_b) and from the initial ~~concentration at the site~~condition (c_i). For the purposes of the network design, the initial ~~concentrations are~~ concentration is ignored since it is assumed that ~~these concentrations are well~~ this condition is constrained by the observations~~and therefore~~. Peylin et al. (2005) found for their European regional inversion that the initial condition had an effect on the flux estimates for only a few days. In a smaller domain, this effect will be even shorter, and therefore it is assumed that the initial condition will contribute very little to the total flux uncertainty.

~~A simple linear relationship can be used to describe~~ The linear relationship used to model the relationship between ~~the modelled concentrations~~ c and the contribution from the sources (~~surface fluxes and boundary inflow)~~ c_s and c_b) is as follows:

$$\boldsymbol{c}_{\text{mod}} = \mathbf{T}\boldsymbol{f} \tag{1}$$

The vector of the modelled concentrations $\boldsymbol{c}_{\text{mod}}$ is a result of the contribution from the sources $\boldsymbol{f}$, described by the transport or sensitivity matrix $\mathbf{T}$. The vector $\boldsymbol{f}$ can be composed of surface fluxes and boundary concentrations (Lauvaux et al., 2012) . The surface fluxes our inversion setup would solve for are the total CO_2 fluxes within a pixel, which we take to be the sum of the biospheric and fossil fuel fluxes. We aim to solve for the total flux since there is not enough information to disentangle these fluxes. In this type of inversion setup, the surface fluxes can be separated into biospheric and fossil fuel fluxes after the inversion run, using additional information regarding either the fossil fuel or biospheric fluxes (Chevallier et al., 2014) . The contribution from the boundaries was first assessed to determine if ~~the~~ its influence on the ~~flux uncertainties~~ observation errors was negligible, in which case the boundary conditions could be excluded from the network design process. We developed an algorithm for assessing the contribution of the boundary concentrations on

the observation error covariance matrix in Section 2.7.

As described in part 1, for the network design approach we are only interested in the posterior covariance matrix of the fluxes, since our aim is to obtain a network that reduces the CO_2 flux uncertainties (Ziehn et al., 2014). The posterior flux error covariance matrix, $\mathbf{C}_f$, can be calculated as follows (Tarantola, 1987):

$$\mathbf{C}_f = \left(\mathbf{T}^T \mathbf{C}_{\mathrm{c}}^{-1} \mathbf{T} + \mathbf{C}_{f_0}^{-1}\right)^{-1} \tag{2}$$

$$= \mathbf{C}_{f_0} - \mathbf{C}_{f_0} \mathbf{T}^T \left(\mathbf{T}\mathbf{C}_{f_0}\mathbf{T}^T + \mathbf{C}_{\mathrm{c}}\right)^{-1} \mathbf{T}\mathbf{C}_{f_0} \tag{3}$$

where $\mathbf{C}_{\mathrm{c}}$ is the covariance matrix of the observation errors, and $\mathbf{C}_{f_0}$ is the prior error covariance matrix of the surface fluxes. ~~The use of the posterior flux covariance matrix to assess uncertainty is possible because it is~~ $\mathbf{C}_f$ is obtained without the vector of observed concentrations $\boldsymbol{c}$ or the vector of prior fluxes $\boldsymbol{f}_0$, which means that it is possible to assess the contribution that a hypothetical station can have on the reduction of the flux uncertainty without the need to generate synthetic data~~or make unnecessary assumptions about the measurements~~.

2.2 Lagrangian Particle Dispersion Model (LPDM)

To determine which sources and how much of each of these sources a measurement site sees at a given moment, the sensitivity matrix $\mathbf{T}$ containing the influence functions is required. ~~This~~ For a regional inversion this matrix can be directly obtained by running ~~an LPDM~~ a Lagrangian particle dispersion model in backward mode. ~~An LPDM~~The particles are released from the measurement locations and travel to the surface and the boundaries (Lauvaux et al., 2008; Seibert and Frank, 2004) . We used the model developed by Uliasz (1994) which we refer to as LPDM. In this mode the model simulates the release of a large number of particles from arbitrary emissions sources by tracking the motion of the particles ~~(Uliasz, 1993, 1994) . The model can be run backward in time, in~~ backward in time (Uliasz, 1993, 1994) . By running the model in this receptor-orientated mode ~~, to calculate~~ the influence functions for a given receptor are calculated, as described in ~~Ziehn et al. (2014) . In this mode, the particles are released from the measurement locations and travel to the surface and the boundaries (Lauvaux et al., 2008; Seibert and Frank, 2004) .~~ part 1 (Ziehn et al., 2014) .

LPDM is driven by the three-dimensional fields of mean horizontal winds (u, v, w), potential temperature and turbulent kinetic energy (TKE). In the case of the South African network design, these variables are produced by the CSIRO Conformal-Cubic Atmospheric Model (CCAM), a variable-resolution global circulation model ~~.~~ run in regional mode. We use the regional mode so that we can resolve the atmospheric transport at a high temporal resolution, which requires that the transport model be run at a high spatial resolution as well (Sarrat et al., 2009) . CCAM uses a two time-level semi-implicit semi-Lagrangian method to solve the hydrostatic primitive equations (McGregor and Dix, 2008; McGregor, 2005; McGregor and Dix, 2001). Total-variation-diminishing vertical advec-

tion is applied to solve for the advective process in the vertical. CCAM employs a comprehensive set of physical parametrisations, including the Geophysical Fluid Dynamics Laboratory (GFDL) parametrisation for long-wave and shortwave radiation (Schwarzkopf and Fels, 1991) and the liquid and ice-water scheme of Rotstayn (1997) for interactive cloud distributions. A canopy scheme is included, as described by Kowalczyk et al. (1994), having six layers for soil temperatures, six layers for soil moisture (solving Richard's equation), and three layers for snow. The cumulus convection scheme uses mass flux closure and includes both downdrafts and detrainment (McGregor, 2003).

In the simulations performed here CCAM is applied in stretched-grid mode by utilising the Schmidt (1997) transformation. A multiple-nudging strategy was followed. First, a modestly-stretched grid providing 60 km resolution over southern and tropical Africa was applied following Engelbrecht et al. (2009), with subsequent downscaling to a strongly-stretched grid providing 15 km resolution over southern Africa. Away from the high-resolution region over southern and tropical Africa, CCAM was provided with synoptic-scale forcing of atmospheric circulation, from the 2.5° (about 250 km) resolution National Centers for Environmental Prediction (NCEP) reanalysis data set. This forcing was provided at 6-hourly intervals for the period 1979-2010 using a scale-selective Gaussian filter (Thatcher and McGregor, 2009, 2010). ~~In the South African case,~~ CCAM was set up so that it produced output at an hourly time step and at a 0.15° spatial resolution over South Africa. The domain extended far beyond the South African border, from 10° South to 40° South and from 0° West to 60° East. Meteorological inputs for LPDM were extracted for two months in 2010; January for Summer and July for Winter. For a four week period during each of these months, LPDM was run for each of the hypothetical measurement sites.

~~We use the LPDM originally proposed by Uliasz (1994) , which we run in reverse mode for each hypothetical measurement station we would like to include in the network design process. In our setup for the model, particles were released every 20 seconds for a total of four weeks for the two selected months and each particle's position was recorded at 15 minute intervals. Particles~~ During processing of the particle count data from LPDM, particles that were near the surface were allocated to a surface grid cell and the total count within each of these was obtained to determine the surface influence or sensitivity. These counts depended on the dimensions and position of these surface grid boxes. The particle counts were used to calculate the source–receptor (s–r) relationship, or influence functions, which form the sensitivity matrix $\mathbf{T}$. Here, we followed Seibert and Frank (2004) to derive the elements of that matrix. As described in ~~Ziehn et al. (2014)~~ part 1 (Ziehn et al., 2014) , we modified the approach of Seibert and Frank (2004) to account for the particle counts which were produced by ~~our~~ LPDM as opposed to the mass concentrations which were outputted by the ~~LPDM~~ transport model in their study. The resulting s–r relationship between the measurement site and source i at time interval n, which provide the elements of the matrix $\mathbf{T}$, is:

$$\frac{\partial \bar{\chi}}{\partial \dot{q}_{in}} = \frac{\Delta T g}{\Delta P} \overline{\left(\frac{N_{in}}{N_{tot}}\right)} \frac{29}{12} \times 10^6, \quad (4)$$

where $\bar{\chi}$ is a volume mixing ratio (receptor) expressed in ppm and $\dot{q}_{in}$ is a mass flux density (source), N_{in} the number of particles in the receptor surface grid from source grid i released at time interval n, ΔT is the length of the time interval, ΔP is the pressure difference in the surface layer, g is the gravity of Earth, and N_{tot} the total number of particles released during a given time interval.

For the network design we are interested in weekly fluxes of carbon separated into day and night time contributions, which means that we have to provide the particle count N_{in} as the sum over one week (ΔT=1 week (day/night)). Therefore, the mass flux density $\dot{q}_{in}$ in Eqn. (4) has units of gC/m^2/week for the day and similarly for the night.

For the standard network design, the surface layer height is set to 50 m which corresponds to approximately 595 Pa (ΔP). If we assume well mixed conditions, then the s–r relationship should be independent of the thickness of the surface layer, as long as the layer is not too deep, as the particle count will be adjusted proportional to the volume of the grid box. Under stable conditions, this may not be the case (Seibert and Frank, 2004). To test if changing the surface grid box height affects the optimal network design, we have included two cases in the sensitivity analysis where the height has been adjusted to 60 m and 75 m. The optimisation routine was run under each of these specifications, holding all other choices ~~the same~~ as for the standard network design.

As for most inversion studies, a compromise needs to be reached between the dimensions imposed on the source regions and the computational resources available ~~(Kaminski et al., 2001; ?)~~ (Kaminski et al., 2001; Lauvaux et al., 20
To ensure that the computational time of each of the optimisation runs was feasible, the spatial resolution of the surface flux grid boxes was set so that the domain was divided into 50 by 25 grid boxes (a resolution of approximately $1.2^\circ \times 1.2^\circ$) for the standard optimal network design. As a sensitivity test, the resolution of the surface grid boxes was adjusted so that there were 72 by 36 grid boxes (a resolution of $0.8^\circ \times 0.8^\circ$) in one case, and to 100 by 50 grid boxes (a resolution of approximately $0.6^\circ \times 0.6^\circ$) in a second, much closer to the original resolution of the transport model. This change in resolution of the surface grid boxes impacts on the sensitivity matrix, increasing the number of elements in the matrix by a factor of two in the medium resolution case and by a factor of four in the high resolution case. It has further consequences for the prior flux covariance matrix, which needs to accommodate this change in source dimensions, increasing its element count by a factor of four for the medium resolution case, and a factor of sixteen in the high resolution case, requiring far more computational resources than the standard case.

2.3 Observation error covariance matrix

Observation errors result in the values of c_{mod} differing from the observed values in c. Sources of these errors include random and systematic measurement errors, which are usually negligible

at an accredited measurement station, transport model errors, and aggregation errors, which are discussed in more detail at the end of this section (Ciais et al., 2010) . Baker (2000) estimated the observation error covariance matrix by comparing the monthly observation means at Mauna Loa to a smoothed line and determining the monthly standard deviations. These values ranged between 0.34 and 0.16 ppm, and so in their case a value of 1 ppm was applied for the standard deviation to each region, with the assumption that most places would have a higher standard deviation than Mauna Loa. It was also assumed that the measurement sites would be independent of one another and no temporal correlation from month to month, so the matrix was assumed to be diagonal. Wu et al. (2013) fitted the standard deviation terms of the observation error covariance matrix to available data for a mesoscale inversion study, and estimated values between 2.9 and and 3.6 ppm.

We ~~assumed a similar standard deviation for the observations as Baker (2000) , but let the elements of the observation error covariance matrix be set at a standard deviation~~ adopted the same observation errors as for the standard case in part 1 of 2 ppm~~for all existing and potential stations, to account for errors in the atmospheric transport modelling. In the Australian test case~~. This value falls within the range of values reported in the literature. The dominant source of observation error represented here is from the transport model. In part 1 (Ziehn et al., 2014) , a sensitivity analysis was conducted by adjusting the error estimate of the observations based on the location of the station. Since there are far fewer existing stations in South Africa from which we can extract data to assess the potential transportation error, we used the same error for all stations. As part of the sensitivity analysis we assessed the impact of increasing the night time observation error uncertainty to 4 ppm to account for ~~the possible~~ known errors in modelling night time atmospheric transport. In atmospheric inversions night time observations are sometimes not considered at all, achieved by drastically increasing the night time observation error uncertainties ~~(?)~~ (Lauvaux et al., 2012) .

The high resolution test case discussed above allows the opportunity to assess the aggregation error as well. This is the error due to the degradation of the spatial resolution from the original resolution of the transport model to a lower resolution that the inversion can accommodate. ~~The modelled concentrations that result from Tf will differ depending on how the source regions are defined (Kaminski et al., 2001)~~ When there is heterogeneity in the surface fluxes and inhomogeneous transport, averaging the surface fluxes to a coarser resolution leads to errors occurring in the modelled concentrations due to the measurement not representing the larger pixels over which the transport is modelled (Kaminski et al., 2001; Ciais et al., 2010) . The aggregation errors ~~can~~ need to be added to the observation errors, as shown by Kaminski et al. (2001) and Tarantola (2005), and ~~need to~~ must be adjusted if the resolution of the problem is changed. To determine the aggregation error in a feasible manner for each of the potential measurement sites, the $0.6^{\circ} \times 0.6^{\circ}$ test case was substituted as the high resolution case in this calculation, where the grid cells of this case fit exactly into the grid cells of the standard low resolution case. ~~Kaminski et al. (2001)~~ This allowed us to follow the method outlined in Kaminski et al. (2001) , who determined that the aggregation error $\mathbf{C}_{c,m}$ can be

calculated as:

$$\mathbf{C}_{c,m} = \mathbf{T}\mathbf{P}_{-}\mathbf{C}_{f_0}\mathbf{P}_{-}^{T}\mathbf{T}^{T}, \tag{5}$$

where $\mathbf{P}_{-} = \mathbf{I} - \mathbf{P}_{+}$ and $\mathbf{P}_{+}$ is the projection matrix which, if multiplied with the prior flux estimates $\mathbf{f}_0$ of the high resolution case, produces the low resolution prior flux estimates in place of the corresponding high resolution estimates. The solution of $\mathbf{C}_{c,m}$ was obtained for each measurement site, and as a conservative approach, the maximum value of the diagonal was assigned as the aggregation error for that measurement site for the standard resolution case. For the medium and high resolution test cases, since aggregation error would certainly exist but presumably get smaller as the resolution approached that of the transport model (Wu et al., 2011) , the aggregation error was reduced according to the increase in number of grid cells. Therefore it was reduced by half for the medium resolution test case, and by a quarter for the high resolution test case.

2.4 Prior flux error covariance matrix

The elements of the prior flux error covariance matrix need to be constructed from the best available knowledge of sources and sinks ~~on~~ at the surface and at the boundaries. Lauvaux et al. (2008) carried out a mesoscale inversion on synthetic data~~and their~~ , where their inversion setup included the contributions from the boundaries as part of the sources they wished to solve for. Their approach for obtaining the boundary elements of the prior flux error covariance matrix was to use modelled values of CO_2 and adjust them for biases based on observed aircraft and tower data that was available for the four day period under assessment. For the prior error covariance matrix of the fluxes, the error was set at 2 gC m^{-2} day^{-1} for the surface fluxes and 4 ppm for the ~~boundaries~~boundary contributions, and they assumed uncorrelated flux errors on the domain (no spatial correlation). This was further developed by Wu et al. (2013) who used available data to fit hyperparameters, which were the variance and correlation lengths of the prior flux and observation error covariance matrices.

The approach of Chevallier et al. (2010) to obtain the elements of the prior flux error covariance matrix was to set the standard deviations of the fluxes proportional to the hetrotrophic respiration flux of land-surface model ORCHIDEE. This is the approach adopted in the case of the South African optimal network design, where we used a recent carbon assessment study by Scholes et al. (2013) which produced monthly maps of gross primary productivity (GPP), net primary productivity (NPP), hetrotrophic respiration (Rh), autotrophic respiration (Ra) and net ecosystem productivity (NEP) for South Africa. Of these products, most confidence lay in the NPP product. Since NEP = NPP − Rh and in a balanced system NEP should be a small flux (Lambers et al., 2008), NPP was used rather than Rh. ~~Following Chevallier et al. (2010) , the~~ The biosphere flux uncertainties for a particular month were estimated using the following simple relationship:

$$\sigma_{\mathrm{NEP}} = \begin{cases} \min(28\,\mathrm{gC/m^2/week},\ \mathrm{NPP}) & \text{if South Africa} \\ \min(28\,\mathrm{gC/m^2/week}, \mathrm{nearest(NPP)}) & \text{if not South Africa} \end{cases} \quad (6)$$

where $\mathrm{nearest(NPP)}$ represents the NPP estimated for the nearest South African grid cell. As a realistic estimate, areas outside of South Africa, which had no estimates available for NPP from the carbon assessment product, were assigned the NPP estimate from the closest South Africa grid cell for a particular month. In this way, pixels to the east of the continent in the Mozambican region had similar flux uncertainties prescribed as for the northern savannah pixels within South Africa, and those on the west of the continent in Namibia had uncertainties prescribed as for the semi-desert pixels in Northern Cape Province of South Africa. This type of interpolation was carried out to avoid adding unnecessary aggregation errors at the South African terrestrial borders, which would occur if a blanket estimate for NPP outside of South Africa was used. ~~The carbon assessment product produced monthly outputs for all the products. These products were converted into daily values.~~ A blanket estimate would lead to artificially large changes in the flux uncertainties between neighbouring pixels, exaggerating aggregation errors for stations near these borders, and conversely null changes in uncertainty between non-South Africa terrestrial pixels. Since Ra and GPP were also available, and NPP = GPP − Ra, day time NPP and night time Ra were obtained by assuming that all the GPP took place during the day, and half of the Ra took place during the day and half at night. This meant that the day time NPP values tended to be larger in magnitude than the night time Ra values, which is what we would expect for the South African systems. ~~The daily values were accumulated to one week to~~ Using this assumption, the monthly estimates for NPP were converted into weekly values, separately for day and night, to give the final uncertainty values used to construct the prior flux error covariance matrix. The day time NPP and night time Ra values used ~~to obtain~~ as proxies for the NEP uncertainties are plotted for July and January (Fig. 1). In South African systems ~~it is expected that~~ much more biological activity occurs during the Summer months compared to the Winter months, with the consequence that the uncertainty during the Summer months is considerably larger.

Since the domain of the network design includes the fossil fuel sources of South Africa, fossil fuel flux uncertainties needed to be derived as well. ~~As forthe Australian test case~~ Previous regional inversions, where the total flux of a source pixel was solved for, had detailed inventory data available for the fossil fuel emissions, and they assumed these were perfectly known (Schuk et al., 2013) . Since this information was not available for South Africa, we had to consider errors in the fossil fuel fluxes. As for part 1 (Ziehn et al., 2014), these uncertainties were derived from the Fossil Fuel Data Assimilation System (FFDAS) (Rayner et al., 2010; Asefi-Najafabady et al., 2014). Ten realisations for the year 2010 were obtained from the FFDAS product at the original resolution of $0.1^\circ \times 0.1^\circ$. The fluxes were aggregated to our network design resolution of $1.2^\circ \times 1.2^\circ$ and then

the variance calculated for each grid cell. Since the emissions from fossil fuels are usually localised, such as those at power plant locations, the variability in the fossil fuel emissions between grid cells is quite large. But, as shown by Ziehn et al. (2014), the effect of aggregating the data smooths the fossil fuel emissions over the network design domain, and this leads to a reduction in the variability between the different realisations of the FFDAS. It also leads to the aggregation errors discussed in 2.2. Figure 2 shows that the uncertainties for the ten realisations based on the original $0.1^\circ \times 0.1^\circ$ resolution have much larger maximums for individual grid cells than the uncertainties calculated for the aggregated fluxes (Fig. 2). The effect of using a higher spatial resolution for the surface grids, closer to the resolution of the transport model, is considered in the sensitivity analyses as discussed above in section 2.2. The fossil fuel uncertainty and NPP surfaces for these higher resolution cases are provided in Fig. 8.

For the standard network design, the prior flux error covariance matrix is estimated as a diagonal matrix, where the diagonal elements are the sum of the variances of the biospheric fluxes and the fossil fuel ~~emissions~~ fluxes for that grid cell~~,~~. The biospheric flux uncertainties were multiplied by the fraction of the grid cell covered by land, separately for day and night. By multiplying with the land fractions we guarantee that the prior uncertainties for coastal grid cells are scaled accordingly and ocean only grid cells are set to zero, since the NEP and fossil fuel products only apply to the land surface. We assumed no correlation in the prior error covariance matrix of the fluxes. This is a necessary assumption since we have no data from which to determine the best correlation lengths. In reality, grid cells with similar biota and under similar climate will have correlated fluxes. Similarly, fluxes from the same source which occur close in time will also be correlated (Chevallier et al., 2010; Wu et al., 2013). Correlation lengths in space and time are difficult to assess, but have a large impact on the estimated fluxes (Lauvaux et al., 2012). Independence is assumed~~and it is hoped that the~~ , which is a more conservative approach for the optimal network design. Eventual data from the implemented network will then help to resolve the flux correlation estimates during the inversion procedure. To determine what impact ~~the assumed~~ assuming positive correlation lengths in the prior flux error covariance matrix could have on the optimal network design, we used the results from Chevallier et al. (2012), and put together a simple correlation structure where it was assumed that temporal correlations for the same grid cell one week apart had a correlation of 0.5 (independent for day and night), decaying to 0.3 at two weeks apart and 0.1 at three weeks apart. Grid cells adjacent to each other had a correlation of 0.3. The interactions between time and space correlations were determined by the Kronecker product of the spatial and temporal correlation matrices (e.g. two grid cells adjacent to each other but one week apart would have a correlation of 0.3×0.5). Therefore correlation lengths were relatively short.

In the network design under the standard case, we kept the uncertainties of the ocean-only grid cells set to zero, since our focus is on reducing the flux uncertainty over land. We ~~want the terrestrial atmospheric measurements to focus on resolving~~ are not seriously assuming that we know the ocean

fluxes perfectly, but for the purposes of this optimal network design, we would prefer if the terrestrial measurements focused on solving for the terrestrial fluxes~~, and to keep the estimation of the ocean fluxes, which are needed to determine the land fluxes during the inversion procedure, as a separate problem.~~. Of course, to run a full inversion, knowledge is needed about the ocean fluxes and this would be obtained through ocean based measurements. The contributions from the ocean can be divided into the 'near-field' and 'far-field'. The far-field contributions are contained within the boundary contributions. The near-field contributions are those within our domain. A sensitivity test was conducted whereby 10% of the maximum land NEP standard deviation was allocated to the ocean grid cells. This uncertainty represents the uncertainty in the ocean productivity models which would be used to obtain prior estimates of ocean fluxes during an inversion, which are similar to the values allocated by Chevallier et al. (2010). A second case was considered where 10% of the nearest land NEP uncertainty was allocated to each ocean grid cell, so that the uncertainties of the ocean grid cells would increase as the uncertainties of nearby land fluxes increased. The purpose of this test case was only to demonstrate the effect implementing a variable ocean uncertainty scheme.

2.5 Optimisation

Three optimisation routines have been used for optimal network design in the literature, namely IO (Patra and Maksyutov, 2002), GA (Rayner, 2004), and simulated annealing (Rayner et al., 1996). ~~The~~ We used the IO routine, as used for ~~the Australian network design (Ziehn et al., 2014) , was used~~ part 1 (Ziehn et al., 2014) , for the standard network design. This method was previously compared to simulated annealing by Patra and Maksyutov (2002) and found to perform as well or better, with significantly less computational cost.

~~In the IO scheme we first obtained the $s-r$ relationship for each of the hypothetical stations. We~~ During the IO procedure we added one station at a time from the candidate list to our base network of two stations and calculated $\mathbf{C}_\mathrm{f}$. We chose the station that resulted in the smallest uncertainty metric and added it to the network, simultaneously removing it from the candidate list. We then repeated the process until we reached ~~the number of instruments we have available (five)~~our target of five stations. The IO procedure provides us with a stepwise progression of the optimal network.

The overall uncertainty in fluxes can be expressed by two different metrics (Rayner et al., 1996). Either through obtaining the trace of $\mathbf{C}_\mathrm{f}$ (J_Ct) or by summing over all the elements of $\mathbf{C}_\mathrm{f}$ (J_Ce):

$$J_\mathrm{Ct} = \sqrt{\sum_{i=1}^{n} C_{f_{ii}}} \tag{7}$$

$J_\mathrm{Ct} = \sqrt{\sum_{i=1}^{n} C_{f_{ii}}}$

$$J_{\mathrm{Ce}} = \sqrt{\sum_{i=1}^{n}\sum_{j=1}^{n} C_{f_{ij}}} \tag{8}$$

where n is the number of elements in the diagonal of $\mathbf{C}_{\mathrm{f}}$. ~~In the first case we consider only the uncertainty of the fluxes estimated at the source regions, ignoring any correlation between~~ The use of equation 8 results in the minimisation of the average variability between surface pixels. Equation 8 is the more accepted metric to calculate uncertainty for network designs, and it results in the ~~regions, which results in minimising the average uncertainty across source regions. In the second case, the~~ minimisation of the uncertainty of the total flux ~~estimate of the target region is considered, since the variance of the sum of a number of variables is equal to the sum of all the elements in the covariance matrix of those variables. There is no clear answer as to which of these is the best metric for the determination of overall uncertainty reduction, so as for~~ over South Africa. As for part 1 (Ziehn et al., 2014) and as used by Rayner et al. (1996), we use J_{Ce} as the uncertainty metric for the standard design. In ~~the South African test~~ our case, because the domain of the transport model contains terrestrial regions outside of South Africa, we only include the elements of $\mathbf{C}_{\mathrm{f}}$ which are within South Africa in the calculation of the uncertainty metric.

As a sensitivity test, the J_{Ct} uncertainty metric ~~replaced~~ was replaced with J_{Ce}. Minimising either ~~during the optimisation~~ of these metrics should result in an optimal network with reduced overall uncertainty in flux estimates across South Africa, but the results could potentially be quite different, particularly if ~~the off-diagonal posterior flux covariance terms are large~~there are large correlations in the posterior flux error covariance matrix.

We evaluated the different networks in terms of their uncertainty reduction:

$$U_R = 1 - \frac{\hat{J}_{\mathrm{Ce}}}{J_{\mathrm{Ce\,base}}} \tag{9}$$

where $\hat{J}_{\mathrm{Ce}}$ is the optimised uncertainty metric value and $J_{\mathrm{Ce\,base}}$ the value of the uncertainty metric ~~based on the posterior uncertainties~~ calculated from the posterior error covariance matrix of the fluxes if only the base stations are included.

Although IO is expected to be more computationally efficient, optimisation through a GA would also be well suited for this kind of problem, considering that this network design for South Africa is starting ~~essentially from scratch~~with so few existing stations. The GA ~~operates by optimising the five member network simultaneously, and~~ begins with each of the solutions in the population containing five stations. Therefore all five stations are optimised simultaneously, rather than sequentially. This method therefore may be more suited to the case where there are multiple deployments, ~~because it could be conceived~~ as we have. It is possible under these circumstances that the best solution for a five ~~member~~ station network in terms of reducing the overall uncertainty for South Africa, may not include the one station which on its own reduces the uncertainty ~~more than any other station~~the most.

The GA is highly parallel and we can therefore take advantage of high performance computing, but the running time of a GA is still higher in comparison to IO.

The approach used to run the GA during the sensitivity analyses is adopted from Rayner (2004). GA procedures are a class of stochastic optimisation procedures for any numerical algorithm which calculates a score based on a function of inputs. In this case the algorithm calculates a score based on the posterior flux error covariance matrix, given a set of stations. A GA does not optimise based on a single solution, but rather by improving a population of solutions, from which a final solution is selected. New members are added to the population through a process of loss of members which are not sufficiently fit (culling), pairwise combination of previous members (cross-over), and random changes to members (mutation). This represents 'survival of the fittest' and pairwise reproduction and mutation in biological populations.

In this implementation of the GA, elitism is maintained by keeping the best solution from the previous population, without making any changes through cross-over or mutation on this member. The algorithm converges once a given number of iterations is reached, or once a convergence criterion is met. The solution with the best fitness criterion is then selected from this population, where the fitness F is calculated as:

$$F = 1 - \frac{r - 0.5}{N} \tag{10}$$

where r is the ordinal ranking of the member and N is the population size, which ~~in the South African test case~~ for our South African case study was taken to be 100 members. A pseudorandom number x is generated and members are then deleted, or culled, if the value of F is less than x. The culling process will remove about 50 % of the population members. These need to be regenerated to get the population back to the required size. Members are selected at random from the remaining population, and based on new pseudorandom ~~number~~numbers, members are duplicated if their fitness score is above this random number. Sampling is with replacement, so the members with the highest fitness have a good chance of being duplicated more than once. This continues until all the culled members have been replaced and the population size is back to N.

The GA requires a trade-off between the diversity in the solutions, ensuring that the algorithm does not get stuck in local extrema, and strong ~~enough~~ selection to ensure that the population moves towards the optimum solution. This is achieved by adjusting the mutation rate; high enough to produce diversity in the solutions, but low enough to ensure that members with high fitness persist and so ensure a tendency towards the optimum solution. From previous work (Rayner, 2004) a good mutation rate for network design was found to be 0.01.

The population size and number of iterations affects the computation time of the algorithm. A large population size is favourable because this ensures diversity in the solutions. The more iterations that take place, the more solutions the algorithm can assess and the better the chance of finding the global minimum. High values for both of these parameters results in long computation times. In this study the number of iterations was set at 100 for a single month optimisation, and to 150 for a

combined month optimisation. These values were determined from GA trials carried out on the data prior to deriving the results for this study.

2.6 Measurement sites

~~The aim of the network design is to find the set of stations that minimizes the flux uncertainty over South Africa.~~ Hypothetical stations were selected from a regular grid over South Africa, resulting in 36 equally spaced locations (Fig. 3)~~. Five new instruments are potentially available for deployment.~~ , from which five stations need to be selected. Ultimately, the exact location of the stations will be determined by practical considerations, such as ~~making use~~ the presence of existing infrastructure~~and~~ , such as communication towers and meteorological stations, available manpower, the relative safety of the instruments, and the accessibility of the sites. The optimal network will be used as a guide ~~towards ideal locations, around which stations will be chosen. For the practical implementation, existing infrastructure will be used as much as possible , such as communication towers or meteorological stations~~ as to which locations are ideal. Once station sites have been chosen, it will be possible to again calculate the posterior flux error covariance matrix based on the exact tower locations, and determine how close to the idealisedbut not the same stations as July uncertainty reduction the implemented network can achieve.

2.7 Influence from outside the modelled domain

Since the surface sources are expressed as fluxes in carbon, the contribution to the concentration at the measurement site is expressed in the amount of carbon seen at the measurement site from a particular source. In the case of the boundary sources (or contributions from outside of the domain) which are given as concentrations, their contributions to the concentration at the measurement site are expressed as a proportion of their concentration, dependent on their influence at the receptor site. Part 1 (Ziehn et al., 2014) showed that the boundary contribution can then be written as:

$$\boldsymbol{c}_{\mathrm{b}\,\mathrm{b,mod}} = \mathbf{M}_{\mathrm{B}}\boldsymbol{c}_{\mathrm{B}} \tag{11}$$

where $\mathbf{M}_{\mathrm{B}}$ is the submatrix of $\mathbf{T}$ for the boundary concentrations, ~~c_{b}~~$\boldsymbol{c}_{\mathrm{B}}$. If the elements of $\mathbf{M}_{\mathrm{B}}$ are large enough it may be necessary to include the boundary ~~conditions~~ concentrations in the network design.

For the network design, four boundaries (north, south, east and west) were used and we calculated the sensitivity of hourly observed concentrations to weekly boundary concentrations. To determine if the ~~boundary influence~~ influence of the boundary concentrations on the observation errors should be included in the network design, we needed to know whether the ~~uncertainty~~ uncertainties contributed by the boundary concentrations were significant compared to other contributions. To see this we calculated $\mathbf{M}_{\mathrm{B}}$ for each station. Assuming ~~concentration~~ uncertainties of 1 ppm ~~at the boundary~~ in

the boundary concentrations (reasonable for the Southern Hemisphere) this yielded:

$$\mathbf{C}_\mathrm{b} = \mathbf{M}_\mathrm{B}\mathbf{C}_\mathrm{I}\mathbf{M}_\mathrm{B}^T \tag{12}$$

where $\mathbf{C}_\mathrm{I}$ is the prior error covariance matrix of boundary concentrations. The diagonal elements of the ~~posterior~~ error covariance matrix of the boundary concentrations, $\mathbf{C}_\mathrm{b}$, provided us with the uncertainty contribution of the boundary concentrations to the observations. If they are much smaller than the observation error uncertainty we can neglect boundary influences in the network design. As the boundary concentrations should be highly correlated, we also considered $\mathbf{C}_\mathrm{I}$ to have correlation between boundary concentrations, where correlations of 0.5 were allocated between boundary concentrations during the same week, and values of 0.25 between boundary concentrations separated by a week or more.

2.8 Comparison of network solutions

To compare the utility of the optimal networks from each algorithm run, the uncertainty reduction was assessed for each of these networks. The similarity of the networks in terms of the station locations was assessed using a test statistic from the Chi-squared Complete Spatial Randomness test, measuring the degree of clustering, where the expected value is based on the null hypothesis that the stations are located randomly over the domain. The intention here was not to perform a statistical test based on the Chi-squared distribution, since the network did not constitute a sample nor were there enough stations, but to calculate an indicator that would assess ~~how similar the positioning of~~ the degree of clustering of the measurements stations ~~were between two networks~~for a particular network solution, referred to as the clustering index, which was also used to compare between two networks.

$$\text{Clustering Index} = \sum_i \sum_j \frac{(O_{ij} - E_{ij})^2}{E_{ij}} \tag{13}$$

where i and j are the indicators for the latitude and longitude categories respectively, O_{ij} was the observed number of stations in quadrat ij and E_{ij} the expected number of stations assuming the stations are scattered randomly. The domain was divided into quadrats; in this case 16 equally sized quadrats covering the entire domain.

A dissimilarity index (DI) was calculated as the sum of the distance to the nearest neighbour in the compared network, over all the members in the pair of assessed networks.

$$DI = \sum_{i=1}^{5} \min \sqrt{\Delta \mathrm{x}_{\mathrm{ij}}^2 + \Delta \mathrm{y}_{\mathrm{ij}}^2} + \sum_{j=1}^{5} \min \sqrt{\Delta \mathrm{x}_{\mathrm{ij}}^2 + \Delta \mathrm{y}_{\mathrm{ij}}^2} \tag{14}$$

where i and j $\in$ [1,2,3,4,5], and $\Delta \mathrm{x}_{\mathrm{ij}}^2$ and $\Delta \mathrm{y}_{\mathrm{ij}}^2$ are the squared differences between the Cartesian coordinates of the ith station in network 1 and the jth station in network 2. In cases where the two networks compared were the same, the index results in a value of zero. The index increases as the

networks become more dissimilar ~~. The reason for using such an index was to produce~~ in space. This provides a one-number measure of network similarity that ~~could~~ can consistently be used for the network comparisons ~~.~~ provided each solution consists of the same number of stations. The index provides a measure in kilometres of how different two network solutions are. This allows for an objective assessment of how different the positioning of sites are between two network solutions which may not be obvious to the eye.

3 Results and Discussion

3.1 Influence from the boundaries

~~As for part 1 (Ziehn et al., 2014) , the LPDM was run for each station, including the two stationsin the existing network . The influence functions for each station for the months of January and July were calculated.~~ The particle counts ~~used to calculate the influence functions~~ generated during the LPDM runs for each station were summed over the month in order to obtain a footprint of each station. To illustrate this, plots of the influence footprint in January (Fig. 4) are provided, using a logarithmic scale, for Cape Point and three other candidate stations~~numbered~~ : 28 (near Potchefstroom), 18 (near Mthatha), and 4 (near Port Elizabeth)~~as examples~~. For both January and July, the influence footprints show that the three candidate stations have more contributions from terrestrial South African sources than Cape Point has. The plots show that the majority of influence for a site is from the sources in the surrounding pixels.

Using the influence functions now available for each station, the test of the influence from the boundaries on to the observation errors was conducted. Given the large domain over which LPDM was run, it was not surprising that the boundaries had minimal influence. Overall, the square root of the maximum diagonal element of $\mathbf{C}_b$ for all stations was only 0.012 ppm. The mean of the maximum diagonal elements over all measurement sites was 0.006 ppm with a standard deviation of 0.002 ppm. Even when correlation between the boundary concentrations was included in the covariance matrix of the boundary concentrations, the maximum diagonal element only reached 0.012 ppm, and ~~maximum diagonal elements~~ the maximum diagonal element for a particular station were no more than 40 % higher than for the independent case.

3.2 Aggregation error

Aggregation errors were found to be a significant contributor to the overall observation error covariance matrix. Aggregation errors of as high as ~~17.1~~17.10 ppm were found for measurement sites in the north eastern interior, and as low as ~~0.0~~0.01 ppm for stations in the south western interior (Fig. 5). The average aggregation error across sites was ~~4.7~~4.70 ppm with a standard deviation of ~~5.1~~5.10 ppm. The sites with the largest aggregation errors were generally those closest to large fossil fuel sources. These large values are due to the significant amount of smoothing of the relatively

localised fossil fuel fluxes during the lower resolution case. This results in large heterogeneity between the high resolution fossil fuel fluxes which contribute to the average fossil fuel flux estimate of the low resolution case, which is exactly the circumstances that lead to the generation of aggregation error. Sites near the terrestrial or coastal borders ~~were also inclined~~ also tended to have large aggregation errors. Site specific aggregation errors were determined, and these errors were added to the ~~observation error uncertainty~~ diagonal elements of the observation error covariance matrix separately for each site.

~~In the specific case of using a backward~~ When running LPDM to generate the sensitivity matrix, it is imperative to specify a sufficient number of particles per release, as well as to ~~allow for enough spin up of the model in order to avoid~~ run the model for longer than required, with additional time at the beginning of the run. This is to avoid transport errors, and to avoid exaggerating the aggregations errors. Therefore, the aggregation errors were calculated using the last week of the four week sensitivity matrix.

The next sections present the results of the optimal network design; first under the basic parametrisations as used in ~~Ziehn et al. (2014)~~ part 1 (Ziehn et al., 2014) , and then under the sensitivity ~~analyses~~tests.

3.3 Basic network design

The network solution for July was able to achieve a reduction in uncertainty in the total South African flux from 6.42 gC/m^2/week under the base network to 3.66 gC/m^2/week under the optimal network. The results under the standard conditions used in the basic network design for the month of July reveal that the best set of stations to add to the current network would include two stations near the western coast of the country, including one just north of the City of Cape Town (Fig. 6). These stations are located near the areas of highest NEP uncertainties during the Winter months. These areas in the Western Cape fall into the fynbos biome, which is under a Winter rainfall regime. Therefore productivity during the Winter months is expected to be higher in this area (Fig.1 a). In contrast, activity over much of South Africa during the Winter months, when water availability is reduced, is expected to be low to almost entirely dormant. Due to the increased uncertainty in NEP in the fynbos regions during this time, as well as the proximity to the City of Cape Town, the optimal network would need a station in this area to reduce the overall uncertainty of South Africa. Two stations are located in the eastern interior of the country, including one on the border of Lesotho, and a station in the central interior of the country, not far from the Zimbabwean border. These stations are located near to areas ~~of~~ with high fossil fuel flux uncertainties. The base network on its own reduced the posterior flux uncertainty by $17.0\,\%$. During the month of July, the best station to add to this network would be station 24, located in the eastern interior of South Africa, just north of Lesotho, which reduced the uncertainty relative to the base network by $12.8\,\%$ (Table. 1). The second best station to add is station 0, near the south east coast of South Africa. This station reduced the uncertainty by an additional $10.5\,\%$. Since the optimal network included a station near

Cape Point during July, it supports the conclusions by Whittlestone et al. (2009) that measurements at Cape Point are not sufficient to estimate fluxes for the Western Cape region. The reduction in uncertainty by the addition of the three remaining stations to the network was an additional 19.3%. During the Winter months, the biospheric fluxes are small, with small uncertainties whereas the fossil fuel flux uncertainties remain high. Due to the penalty imposed by the aggregation error for measurement sites located near fossil fuel sources, the return on uncertainty reduction during the Winter months is low, at only 42.9%.

In January the ~~picture changed, with the stations~~ total flux uncertainty was much higher compared to July, with a total flux uncertainty of 128 gC/m^2/week, which was reduced to 27.93 gC/m^2/week under the optimal network. The placement of stations changes with respect to July, with the stations all located towards the eastern interior of the country, and no stations positioned on the western side of South Africa (Fig. 6). The stations were located near regions of high Summer time NEP uncertainty and in the region where most of the fossil fuel activities in the country are concentrated. In contrast to the Winter months, the NEP uncertainty during Summer is much higher on the eastern side of the country compared to the mid interior or the west of the country (Fig.1 c), resulting in a need to concentrate the new measurement sites in this area. The uncertainty reduction attributable to the base network in January is similar to July, at 16.8%. The best performing station in the network for January is station 12, located on the eastern coast of South Africa, which further reduces the uncertainty by 40.0% relative to the base network. The next best performing station was station 29, which reduced the uncertainty by an additional 18.0%. An additional 10.3% increase in uncertainty reduction was attained from adding the last three stations to the network. The total uncertainty reduction achieved in January is much higher compared to July, at 78.3%. This is due to the ability of the network to view the larger Summer biospheric fluxes in areas where the aggregation error penalty is low, or even despite the aggregation error penalty.

The total flux uncertainty under the base network for the combined months of January and July ~~result in~~ was calculated to be 128.43 gC/m^2/week, similar to the month of January. This is reduced to 19.83 gC/m^2/week under the optimal network. The network for the combined months has a similar positioning of stations compared to January (Fig. 6), locating most of the stations in the eastern interior, as well as a very similar reduction in uncertainty at 84.6%. The most important station, as ranked by the IO solution, is station 18, which reduces the uncertainty by 53.3% relative to the base network. This station is located in a region of both high NEP and fossil fuel flux uncertainty (Fig. 1 and Fig. 2). The second best station to add to the network is station 29, increasing the uncertainty reduction by 24.4%. This station is located near the area of highest fossil fuel flux uncertainty (Fig. 2). The remaining three stations (stations 11, 22 and 27) add only 6.8% to the uncertainty reduction. The network solution is different to January's, in that the stations are more concentrated around the areas of larger fossil fuel flux uncertainty. This is due to the much lower NEP uncertainty estimates for the Winter months across South Africa compared to the Summer months, but the fossil fuel flux

uncertainties remaining consistent during the year. The optimal network for the combined seasons is therefore dominated by the need to reduce these consistently large uncertainties. The results from the combined months shows that a substantial reduction in the posterior uncertainty for South Africa is possible by introducing only a few additional stations at key locations.

3.4 Sensitivity analysis

The results for the sensitivity analyses run for both months, and the combined months of January and July appear in Fig. 7. During the Winter months, there was consistency between the network solutions from the different sensitivity tests. All of the tests were in agreement that stations 0 and 18 should be included; station 0 near the Winter NEP uncertainties, and station 18 near an area of large fossil fuel flux uncertainty. The tests assessing surface grid box height, the doubling of night time observation error uncertainty, and the addition of ocean flux uncertainty, were identical to the standard network design solution. Both the medium resolution and the GA network solutions were very near the standard solution, each obtaining the second smallest DI relative to the standard design of 879. These tests both favoured two stations which were each one step away from a standard network design station. The solution using the uncertainty metric based on the trace of the posterior flux covariance matrix was similar to these two, but favoured a station near the south coast of South Africa, far from the general concentration of stations, near a localised fossil fuel source. The two test cases most different from the standard solution were the high resolution network solution, and the solution from the case considering correlation between the prior fluxes, obtaining a DI of 1747 and 1343 respectively. They also favoured ~~networks~~ stations near the south coast, but also located stations in the north eastern interior, near areas of large fossil fuel uncertainty.

The results from the sensitivity tests for January show a great deal more variability between network solutions compared to July, with DI values of greater than zero for almost all network solution comparisons. Similarly to July, the network solutions do appear to converge towards three stations, but not the same stations as July. Under January's conditions, only the homogeneous ocean variance test case resulted in an identical solution to the standard case. There is no single station which all network solutions contained. Stations 29 (north eastern interior) and station 12 (eastern coast) were agreed on by ten out of eleven tests, and stations 27 (northern interior) and 11 (south eastern interior) were agreed on by nine out of eleven tests. These four stations are influenced by areas of large fossil fuel flux uncertainty, and stations 29 and 12 near regions or large Summer NEP uncertainty. Sensitivity tests with DI values below 1000 when compared to the standard case include the tests considering surface grid box height, doubling of night time observation error uncertainty, the test considering variable ocean flux uncertainty, the trace uncertainty metric test, and the GA test case. These five test cases show strong agreement. The trace uncertainty metric case favoured a station near the central interior. This station was also included in the solutions of the correlation and medium resolution cases, where these tests obtained DI values of 1225 and 1305 respectively when

compared to the standard solution. These tests, as well as the GA and high resolution test cases, included stations near the south coast, near areas of localised fossil fuel uncertainties.

The sensitivity tests from the combined months showed less variability between solutions compared to January (Fig.7 c). Station 11 was included in all of the network solutions. Station 18 was agreed upon by ten out of eleven network solutions, and stations 27 and 29 (both in the north eastern interior) were favoured by nine out of eleven solutions. The tests considering 60 m surface height, the trace uncertainty metric, doubling of the night time observation error uncertainty, and inclusion of ocean flux uncertainty have identical solutions to the standard network design. The 75 m surface height and medium resolution tests cases obtained relative low DI values of 468 and 449 respectively when compared to the standard solution (Table 2). The high resolution test and test case considering correlation between prior fluxes obtained DI values of 1121 and 1162 respectively. The solutions from these tests focused stations around areas of large fossil fuel flux uncertainty in the north western and eastern interior. The solution from the GA resulted in the largest DI value of 1213 when compared to the standard network, and equal to this or larger when compared to all other network solutions. The station in the GA solution responsible for the disagreement with other solutions is station 7, located in the south western interior, far from the concentration of stations ~~from~~ for most network solutions. The remaining four stations from the GA test are located ~~in this region,~~ towards the north western and eastern interior parts of the country. As discussed in the previous section (3.3) the three best stations to add to the network according to the IO solution, are stations 18, 29 and 11, with station 18 attaining the greatest uncertainty reduction. All of the network solutions for the combined months of January and July have included station 18, and the three most important stations are all in the solution of the GA.

The statistics for the different sensitivity tests for the combined months (Table 3) indicate that the test considering correlation between the prior fluxes obtained the highest uncertainty reduction, followed by the GA test. The GA was able to achieve marginally greater uncertainty reduction by 0.3% compared to the IO standard solution. Most of the test cases were able to achieve between 80% and 85% uncertainty reduction. The test case utilising the trace uncertainty metric achieved a smaller uncertainty reduction, and the two higher resolution tests achieved the smallest uncertainty reduction overall. Estimates of the posterior uncertainty for the total flux of South Africa under the base and optimal networks were obtained for each month. Those which differed substantially from the standard network solution were the high and medium resolution test cases, and the correlation test case. Under the assumption of positive correlations between the flux errors, the base network results in a higher total flux uncertainty of 205.82 gC/m^2/week for the base network which is reduced to 27.79 gC/m^2/week under the optimal network, now similar to the result of the standard network solution. Under the base network, the additional covariance terms introduced through the correlation structure are poorly resolved, leading to higher total uncertainties. When there are more stations added to the network this is improved. The high and medium spatial resolution test cases gave total

flux uncertainties of 271.55 and 190.14 gC/m^2/week respectively under the base network. These were then reduced to 82.82 and 44.19 gC/m^2/week respectively under the optimal network. At the spatial resolutions that we've considered in our study, the between pixel variability in the terrestrial fluxes will increase as the spatial resolution is increased, for both the biospheric and fossil fluxes (Turner et al., 2000) . For the fossil fuel fluxes, we create the surface of flux uncertainties using the same procedure for each of the different spatial resolution cases. As explained earlier, for each of the ten realisations from the FFADS product, we regrid the $0.1^\circ \times 0.1^\circ$ fossil fuel emissions onto the surface grid we are using. To obtain the uncertainty estimates the within pixel variance is calculated for the ten realisations. The result of carrying this procedure out at higher spatial resolutions is that the variance values are larger compared to lower resolutions, and the between pixel variability is increased (Asefi-Najafabady et al. 2014). Therefore, the total flux uncertainty derived under a high resolution is expected to be larger than for lower resolutions.

Most network solutions tended towards the same amount of clustering of stations, obtaining a clustering index of 23.8. The GA and test case considering correlation had more dispersed networks, and the high resolution test case had the highest amount of clustering, with a clustering index of 36.6. We would expect the correlation case to spread stations since a given station will reduce uncertainty everywhere within one correlation length. The GA for the combined months took the longest to run, at over 32 hours, which is 39 times longer than the running time of the standard IO solution. This was followed by the high resolution solution, which took 25.2 hours, and the two ocean flux uncertainty test cases which took over five hours each.

4 Summary and Conclusions

Under a reference set of conditions, an optimal network design was obtained for South Africa for two representative months of the year. The resulting designs reduced the uncertainty of carbon fluxes from South Africa compared to the base network by $43\,\%$ in July and $78\,\%$ in January. These relatively large reductions in uncertainty are due to the lack of coverage by the current network, which only reduces the uncertainty of fluxes from South Africa by $16\,\%$ for both July and January. The concentration of stations by all networks tended towards the central interior, near the North West Province of South Africa and in the eastern parts of the country. These represent the areas with the largest uncertainty in biospheric fluxes, as well as fossil fuel emissions, in the country.

Station 11 is located near the uKhahlamba Drakensberg World Heritage Site. Several remote holiday destinations occur in this area, near the town of Mooi River, and road infrastructure is available. Potentially, facilities at or near these holiday destinations could be utilised in order to conduct atmospheric measurements, particularly if there is a communications tower available. Station 18 is located near the peak of Ben Macdhui. This is near the site of a 1996 atmospheric monitoring campaign, which assessed the ability of transport models to resolve recirculation over and exiting South

Africa to the Indian Ocean (Piketh et al., 1999). Station 29 is near the atmospheric monitoring site of the North West University (South Africa), at Welgegund, about 20 km from the Potchefstroom campus. This site was established in collaboration with the University of Helsinki to measure the impact of aerosols and trace gases on the climate and air quality (Tiitta et al., 2014). Therefore, for at least three of the most influential stations, facilities or previous measurement campaigns exist, indicating that it should be possible to establish long term monitoring of CO_2 concentrations near these sites.

The sensitivity analysis demonstrated that for most of the network design parameters considered in this study, the stations found to be most important by the standard network design were always identified in the network design solution. Many of the choices required for the optimal network design, such as the height of the surface grid cells, whether to inflate night time observation error uncertainties relative to the day time, and the inclusion of ocean flux uncertainty, have a negligible impact on the final network design. Substituting the trace for the sum of the covariance elements also resulted in similar solutions.

The test cases considering higher spatial resolution tended to result in network solutions different from the standard case, largely due to the increase in spatial heterogeneity in prior flux uncertainties compared to the coarser resolution. The spatial resolution of an inversion study impacts network design in several ways. It is the main determinant of the amount of aggregation error attributed to a measurement site, with aggregation error reducing as the resolution increases. As the spatial resolution is degraded, aggregation errors can become large, leading to the exclusion of sites in the case of an optimal network design, even if they are in view of regions of large flux uncertainty. The ~~resolution~~ spatial resolution of the sources also determines the ~~size~~ dimensions of the sensitivity matrix and prior flux covariance matrix, which impacts on the computational resources required to run an inversion or network optimisation. Ideally, the highest manageable resolution should be used, as close as possible to the resolution of the transport model and original spatial products used for obtaining the prior fluxes and their covariances. Alternative approaches, such as the use of multi-scale representation of the source region can be used to mitigate aggregation errors as well (Wu et al., 2011) , but these errors should always be considered during an inversion or inversion-based optimal network design exercise.

The GA was able to find marginally better solutions than the IO method, if run with sufficient population size and number of iterations, but in general did include the most influential stations from the IO solution. The increase in uncertainty reduction was found to be marginal, but cost a great deal more in running time before this solution was found. If the resolution of the standard case had been higher, the GA would have taken longer to run, and the current computing system may have had insufficient memory. Moreover, to find a better solution than the IO, the iterations and population size would have had to be set even higher, due to the greater heterogeneity in the prior flux uncertainties in a higher resolution setup, further increasing the computational costs. An additional

advantage of the IO method over the GA method is that an evolution of results is generated, which is useful for practical purposes. By identifying the station which on its own best reduces the uncertainty in the posterior fluxes, it gives the decision makers the location of the site which should be prioritised over others in the network.

~~Since~~ Even though we accounted for aggregation error, which would have corrected the total flux estimate for the domain, there were still large differences between the total flux uncertainties from the inversion results under different spatial resolutions. This was due to the treatment of the prior uncertainties under the different spatial resolutions. Degrading the spatial resolution results in a loss of information, therefore it is best to run the inversion at as high a resolution as possible~~,~~ ~~favouring~~ . Favouring optimisation techniques like IO, which can more easily accommodate high spatial resolution, over those which could force a reduction in resolution due to high computational demands, such as the GA, may be unavoidable. Techniques like ~~the GA and simulated annealing~~ simulated annealing and the GA do not guarantee the global optimum, as demonstrated by Patra and Maksyutov (2002) ~~and in this study, during the lead up to the use~~ for simulated annealing and during the initial trials of the GA in this study. Patra and Maksyutov (2002) also showed that as the number of stations in the network increased, the performance of simulated annealing relative to the IO decreased, with IO eventually achieving significantly better uncertainty reductions.

Of the sensitivity tests, including correlation had one of the largest impacts on the final network result, often differing significantly from the standard solution. The correlation structure used in this study was generic, simply assuming that fluxes from nearby grid cells and fluxes at the same location near in time would be correlated, included for the purpose of assessing the impact of correlation in the prior fluxes. For a network to be based on a prior covariance matrix including correlation, there would need to be confidence that this correlation structure and size of correlations between fluxes were accurate. This is generally not the case, and easier to assess when concentration measurements are available, which is why many network designs have assumed independence between prior fluxes (Rayner, 2004; Patra and Maksyutov, 2002). Including correlations which are too large can lead to an over constrained system (Lauvaux et al., 2012), which is evidenced in this study where the uncertainty reductions were the largest under the correlation test case.

Overall the results suggest that a good improvement in knowledge of South African fluxes is achievable from a feasible atmospheric network and that the general features of this network are invariable under many reasonable choices in a network design study.

Acknowledgements. Peter Rayner is in receipt of an Australian Professorial Fellowship (DP1096309). This worked was supported by parliamentary grant funding from the Council of Scientific and Industrial Research. The authors would like to thank the helpful commentary from Thomas Lauvaux on the implementation and post processing of the LPDM.

References

Asefi-Najafabady, S., Rayner, P. J., Gurney. K. R., McRobert, A., Song, ., Coltin K., Huang, J., Elvidge, C., and Baugh, K.: A multiyear, global gridded fossil fuel CO_2 emission data product: Evaluation and analysis of results, J. Geophys. Res., 119, doi: 10.1002/2013JD021296, 2014

Baker, D. F.: An inversion method for determining time-dependent surface CO2 fluxes, in: Kasibhatla, P., Heimann, M., Rayner, P., Mahowald, N., Prinn, R. G., and Hartley, D. E., (Eds.): Inversion methods in global biogeochemical cycles, Geophysical Monograph 114, American Geophysical Union, 279–293 Washington D.C., USA, 2000

Baker, D. F., Law, R. M., Gurney, K. R., Rayner, P., Peylin, P., Denning, A. S., Bourquet, P., Bruhwiler, L., Chen, Y., Ciais, P., Fung, I. Y., Heimann, M., John, J., Maki, T., Maksyutov, S., Masarie, K., Prather, M., Pak, B., Taguchi, S., Zhu, Z.: TransCom 3 inversion intercomparison: impact of transport model errors on the interannual variability of regional CO_2 fluxes, 1988–2003, Global Biogeochem. Cy., 20, GB1002, doi: 10.1029/2004GB002439, 2006.

Bousquet, P., Ciais, P., Peylin, P., Ramonet, M., and Monfray, P.: Inverse modeling of annual atmospheric CO_2 sources and sinks: 1. Method and control inversion, J. Geophys. Res., 104, 26161–26178, 1999.

Canadell, J. G., Le Quéré, C., Raupach, M. R., Field, C. B., Buitenhuis, E. T., Ciais, P., Conway, T. J., Gillett, N. P., Houghton, R. A., and Marland, G.: Contributions to accelerating atmospheric CO_2 growth from economic activity, carbon intensity, and efficiency of natural sinks, P. Natl. Acad. Sci. USA, 104, 18866–18870, doi: 10.1073/pnas.0702737104, 2007.

Chevallier, F., Ciais, P., Conway, T. J., Aalto, T., Anderson, B. E., Bousquet, P., Brunke, E. G., Ciattaglia, L., Esaki, Y., Fröhlich, M., Gomez, A., Gomez-Pelaez, A. J., Haszpra, L., Krummel, P. B., Langenfelds, R. L., Leuenberger, M., Machida, T., Maignan, F., Matsueda, H., Morgui, J. A., Mukai, H., Nakazawa, T., Peylin, P., Ramonet, M., Rivier, L., Sawa, Y., Schmidt, M., Steele, L. P., Vay, S. A., Vermeulen, A. T., Wofsy, S., and Worthy, D.: CO_2 surface fluxes at grid point scale estimated from a global 21 year reanalysis of atmospheric measurements, J. Geophys. Res., 115, D21307, doi: 10.1029/2010JD013887, 2010.

Chevallier, F., Wang, T., Ciais, P., Maignan, F., Bocquet, M., Arain, M. A., Cescatti, A., Chen, J., Dolman, A. J., Law, B. E., Margolis, H. A., Montagnani, L., and Moors, E. J.: What eddy-covariance measurements tell us about prior land flux errors in CO_2-flux inversion schemes, Global Biogeochem. Cy., 26, GB1021, doi: 10.1029/2010GB003974, 2012.

Chevallier, F., Palmer, P. I., Feng, L., Boesch, H., O'Dell, W., and Bousquet, P.: Toward robust and consistent regional CO_2 flux estimates from in situ and spaceborne measurements of atmospheric CO_2, Geophys. Res. Lett., 41, 1065–1070, doi:10.1002/2013GL058772, 2014.

Ciais, P., Rayner, P., Chevallier, F., Bousquet, P., Logan, M., Peylin, P., and Ramonet, M.: Atmospheric inversions for estimating CO_2 fluxes: methods and perspectives, Climatic Change, 103, 69–92, 2010.

Denman, K. L., Brasseur, G., Chidthaisong, A., Ciais, P., Cox, P. M., Dickinson, R. E., Hauglustaine, D., Heinze, C., Holland, E., Jacob, D., Lohmann, U., Ramachandran, S., da Silva Dias, P. L., Wofsy, S. C., and Zhang, X.: Couplings between changes in the climate system and biogeochemistry, in: Climate Change 2007: The Physical Science Basis. Contribution of Working Group I to the Fourth Assessment Report of the Intergovernmental Panel on Climate Change, edited by: Solomon, S., Qin, D., Manning, M., Chen, Z., Marquis, M., Averyt, K. B., Tignor, M., and Miller, H. L., Cambridge University Press, Cambridge, UK and

New York, NY, USA, 499–587, 2007.

Engelbrecht, F. A., McGregor, J. L. and Engelbrecht, C. J.: Dynamics of the conformal-cubic atmospheric model projected climate-change signal over southern Africa, Int. J. Climatol., 29, 1013-1033., doi: 10/1002/joc.1742.29., 2009.

Enting, I. G.: Inverse Problems in Atmospheric Constituent Transport, Cambridge Univ. Press, New York, 2002.

Enting, I. G. and Mansbridge, J. V.: Seasonal sources and sinks of atmospheric CO_2: direct inversion of filtered data, Tellus B, 41, 111–126, 1989.

Gurney. K. R., Law, R. M., Denning, A. S., Rayner, P. J., Baker, D., Bousquet, P., Bruhwiler, L., Chen, Y., Ciais, P., Fan, S., Fung, I. Y., Gloor, M., Heimann, M., Higuchi, K., John, J., Maki, T., Maksyutov, S., Masarie, K., Peylin, P., Prather, M., Pak, B. C., Randerson, J., Sarmiento, J., Taguchi, S., Takahashi, T., and Yuen, C.: Towards robust regional estimates of CO_2 sources and sinks using atmospheric transport models, Nature, 405, 626–630, 2002.

Gurney, K. R., Law, R. M., Denning, A. S., Rayner, P. J., Baker, D., Bousquet, P., Bruhwiler, L., Chen, Y., Ciais, P., Fan, S., Fung, I. Y., Gloor, M., Heimann, M., Higuchi, K., John, J., Kowalczyk, E., Maki, T., Maksyutov, S., Peylin, P., Prather, M., Pak, B. C., Sarmiento, J., Taguchi, S., Takahashi, T., and Yuen, C.: TransCom 3 CO_2 inversion intercomparison: 1. Annual mean control results and sensitivity to transport and prior flux information, Tellus B, 55, 555–579, 2003.

Kaminski, T., Heimann, M., and Giering, R.: A coarse grid three dimensional global inverse model of the atmospheric transport, 2. Inversion of the transport of CO_2 in the 1980s, J. Geophys. Res., 104, 18555–18581, 1999.

Kaminski, T., Rayner, P J., Heimann, M., and Enting, I. G.: On aggregation errors in atmospheric transport inversions, J. Geophys. Res., 106, 4705–4715, 2001.

Kowalczyk, E. A., Garratt, J. R. and Krummel, P. B.: Implementation of a soil-canopy scheme into the CSIRO GCM - regional aspects of the model response, CSIRO Div. Atmospheric Research, Melbourne, Australia, Tech Paper No. 32, 59 pp., 1994.

Lambers, H., Chapin, F. S., and Pons, T. L.: Plant Physiology Ecology, Springer Science+Business Media L. L. C., New York, USA, 634 pp., 2008.

Lauvaux, T., Uliasz, M., Sarrat, C., Chevallier, F., Bousquet, P., Lac, C., Davis, K. J., Ciais, P., Denning, A. S., and Rayner, P. J.: Mesoscale inversion: first results from the CERES campaign with synthetic data, Atmos. Chem. Phys., 8, 3459–3471, doi: 10.5194/acp-8-3459-2008, 2008.

Lauvaux, T., Schuh, A. E., Uliasz, M., Richardson, S., Miles, N., Andrews, A. E., Sweeney, C., Diaz, L. I., Martins, D., Shepson, P. B., and Davis, K. J.: Constraining the CO_2 budget of the corn belt: exploring uncertainties from the assumptions in a mesoscale inverse system, Atmos. Chem. Phys., 12, 337–354, doi: 10.5194/acp-12-337-2012, 2012.

Lauvaux, T., Schuh, A. E., Bouquet, M., Wu, L., Richardson, S., Miles, N., and Davis, K. J.: Network design for mesoscale inversions of CO_2 sources and sinks, Tellus, 64B, doi:10.3402/tellusb.v64i0.17980, 2012.

Law, R. M., Chen, Y., Gurney, K. R., and Transcom 3 Modellers: TransCom 3 CO_2 inversion intercomparison: 2. Sensitivity of annual mean results to data choices, Tellus B, 55, 580–595, 2003.

McGregor, J. L.: A new convection scheme using a simple closure, in: Current issues in the parameterization of convection, BMRC, Melbourne, Australia, Research Report 93, 33-36, 2003.

McGregor, J. L.: C-CAM: Geometric aspects and dynamical formulation, CSIRO Div. Atmospheric Research, Melbourne, Australia, Tech Paper No. 70, 43 pp., 2005.

McGregor, J. L. and Dix, M. R.: The CSIRO conformal-cubic atmospheric GCM, in: IUTAM Symposium on Advances in Mathematical Modelling of Atmosphere and Ocean Dynamics, Limerick, Ireland, 2–7 July 2000, edited by: Hodnett, P. F., Kluwer, Dordrecht, 197–202, 2001.

McGregor, J. L. and Dix, M. R.: An updated description of the Conformal-Cubic Atmospheric Model, in: High Resolution Numerical Modelling of the Atmosphere and Ocean, edited by: Hamilton, K. and Ohfuchi, W., Springer, New York, USA, 51–76, 2008.

Morgan, E., Lavrič, J., Seely, M., and Heimann, M.: Establishment of an atmospheric observatory for trace gases and atmospheric oxygen in Namibia, Geophys. Res. Abstr., 14, 5122–5122, 2012.

Patra, P. K. and Maksyutov, S.: Incremental approach to the optimal network design for CO_2 surface source inversion, Geophys. Res. Lett., 29, 1459, doi:10.1029/2001GL013943, 2001.

Peylin, P., Baker, D., Sarmiento, J., Ciais, P., and Bousquet, P.: Influence of transport uncertainty on annual mean and seasonal inversions of atmospheric CO_2 data, J. Geophys. Res., 107, 4385, doi: 10.1029/2001JD000857, 2002.

Peylin, P., Rayner, P. J., Bousquet, P., Carouge, C., Hourdin, F., Heinrich, P., Ciais, P., and AEROCARB contributors: Daily CO_2 flux estimates over Europe from continuous atmospheric measurements: 1, inverse methodology, Atmos. Chem. Phys., 5, 3173–3186, doi:10.5194/acp-5-3173-2005, 2005.

Piketh, S. J., Swap, R. J., Anderson, C. A., Freiman, M. T., Zunckel, M., and Held, G.: Ben Macdhui high altitude trace gas and aerosol transport experiment, S. Afr. J. Sci., 95, 35–43, 1999.

Rayner, P. J.: Optimizing CO_2 observing networks in the presence of model error: results from TransCom 3, Atmos. Chem. Phys., 4, 413–421, doi: 10.5194/acp-4-413-2004, 2004.

Rayner, P. J., Enting, I. G., and Trudinger, C. M.: Optimizing the CO_2 observing network for constraining sources and sinks, Tellus B, 48, 433–444, 1996.

Rayner, P. J., Enting, I. G., Francey, R. J., and Langenfelds, R. L.: Reconstructing the recent carbon cycle from atmospheric CO_2, $\delta^{13}C$ and O_2/N_2 observations, Tellus B, 51, 213–232, 1999.

Rayner, P. J., Raupach, M. R., Paget, M., Peylin, P., and Koffi, E.: A new global gridded data set of CO_2 emissions from fossil fuel combustion: mehodology and evaluation, J. Geophys. Res., 115, D19306, doi: 10.1029/2009JD013439, 2010.

Rödenbeck, C., Houweling, S., Gloor, M., and Heimann, M.: CO_2 flux history 1982–2001 inferred from atmospheric data using a global inversion of atmospheric transport, Atmos. Chem. Phys., 3, 1919–1964, doi: 10.5194/acp-3-1919-2003, 2003.

Rotstayn, L. D.: A physically based scheme for the treatment of stratiform clouds and precipitation in large-scale models. I: Description and evaluation of the microphysical processes, Q. J. R. Meteorol. Soc., 123, 1227–1282, 1997.

Sarrat, C., Noilhan, J., Lacarrère, P., Ceschia, E., Ciais, P., Dolmon, A. J., Elbers, E. J., Gerbig, C., Gioli, B., Lauvaux, T., Miglietta, F., Neininger, B., Ramonet, M., Vellinga, O., and Bonnefond, J. M.: Mesoscale modelling of the CO_2 interactions between the surface and the atmosphere applied to the April 2007 CERES field experiment, Biogeosciences, 6, 633–646, doi:10.5194/bg-6-633-2009, 2009.

~~Schmidt, F.: Variable fine mesh in spectral global model, Beitr.~~Schmidt, F.: Variable fine mesh in spectral global

model, Beitr. Phys. Atmos., 50, 211–217, 1977.

~~Schwarzkopf, M. D.and Fels, S. B.: The simplified exchange method revisited: An accurate, rapid method for computation of infrared cooling rates and fluxes, J.Geophys. Res. , 96, 9075–9096, 1991.~~

Scholes, R. J., von Maltitz, G. P., Archibald, S. A., Wessels, K., van Zyl, T., Swanepoel, D., and Steenkamp, K.: National Carbon Sink Assessment for South Africa: First Estimate of Terrestrial Stocks and Fluxes, CSIR Technical Report, Pretoria, South Africa, CSIR/NRE/GC/ER/2013/0056/B, 2013.

Schuh, A. E., Lauvaux, T., West, T. O., Denning, A. S., Davis, K., J., Miles, N., Richardson, S., Uliasz, M., Lokupitiya, E., Cooley, D., Andrews, A., and Ogle, S.: Evaluating atmospheric CO_2 inversions at multiple scales over a highly inventoried agricultural landscape, Glob. Change Biol., 19, 1424–1439, doi: 10.1111/gcb.12141, 2013.

Schwarzkopf, M. D. and Fels, S. B.: The simplified exchange method revisited: An accurate, rapid method for computation of infrared cooling rates and fluxes, J. Geophys. Res., 96, 9075–9096, 1991.

Seibert, P. and Frank, A.: Source-receptor matrix calculation with a Lagrangian particle dispersion model in backward mode, Atmos. Chem. Phys., 4, 51–63, doi: 10.5194/acp-4-51-2004, 2004.

Tarantola, A.: Inverse Problem Theory and Methods for Model Parameter Estimation, Society for Industrial and Applied Mathematics , Philadelphia, 1987.

Tarantola, A.: Inverse Problem Theory: Methods for Data Fitting and Model Parameter Estimation, Elsevier, Amsterdam, 1987.

Thatcher, M. and McGregor, J. L.: Using a scale-selective filter for dynamical downscaling with the conformal cubic atmospheric model, Mon. Weather Rev., 137, 1742–1752, 2009.

Thatcher, M. and McGregor, J. L.: A technique for dynamically downscaling daily-averaged GCM datasets over Australia using the Conformal Cubic Atmospheric Model, Mon. Weather Rev., 139, 79–95, 2010.

Tiitta, P., Vakkari, V., Croteau, P., Beukes, J. P., van Zyl, P. G., Josipovic, M., Venter, A. D., Jaars, K., Pienaar, J. J., Ng, N. L., Canagaratna, M. R., Jayne, J. T., Kerminen, V. -M., Kokkola, H., Kulmala, M., Laaksonen, A., Worsnop, D. R., and Laakso, L.: Chemical composition, main sources and temporal variability of PM_1 aerosols in southern Africa grassland, Atmos. Chem. Phys., 14, 1909–1927, doi: 10.5194/acp-14-1909-2014, 2014.

Turner, D. P., Cohen, W., B., and Kennedy, R. E.: Alternative spatial resolutions and estimation of carbon flux over a managed forest landscape in Western Oregon, Landsc. Ecol., 15, 441–452, 2000.

Uliasz, M.: The atmospheric mesoscale dispersion modeling system, J. Appl. Meteorol., 31, 139–149, 1993.

Uliasz, M.: Lagrangian particle modeling in mesoscale applications, in: Environmental Modelling II, Computational Mechanics Publications, Southampton, UK, 71–102, 1994.

Whittlestone, S., Kowalczyk, E., Brunke, E. G., and Labuschagne, C.: Source Regions for CO_2 at Cape Point Assessed by Modelling 222Rn and Meteorological Data, Technical Report for the South African Weather Service, Pretoria, South Africa, 2009.

Wu, L., Bocquet, M., Lauvaux, T., Chevallier, F., Rayner, P. J. and Davis, K.: Optimal representation of source-sink fluxes for mesoscale carbon dioxide inversion with synthetic data, J. Geophys. Res., 116, D21304, doi:10.1029/2011JD016198, 2011.

Wu, L., Bocquet, M., Chevallier, F., Lauvaux, T., and Davis, K.: Hyperparameter estimation for uncertainty quantification in mesoscale carbon dioxide inversions, Tellus B, 65, 20894, doi: 10.3402/tel-

lusb.v65i0.20894, 2013.

Ziehn, T., Nickless, A., Rayner, P. J., Law, R. M., Roff, G., and Fraser, P.: Greenhouse gas network design using backward Lagrangian particle dispersion modelling - Part 1: Methodology and Australian test case, Atmos. Phys. Chem., 14, 9363-9378, 2014.

Table 1: Ranking of the new stations added to the base network for two seasons (Winter and Summer) represented by July and January, as well as the integrated two months. The cumulative reduction of uncertainty relative to the base uncertainty is provided in brackets.

Rank	July	January	July + January
1	24 (12.8 %)	12 (40.0 %)	18 (53.3 %)
2	0 (23.3 %)	29 (58.0 %)	29 (77.7 %)
3	21 (33.0 %)	11 (68.0 %)	11 (80.9 %)
4	18 (38.1 %)	21 (74.5 %)	22 (82.6 %)
5	6 (42.9 %)	24 (78.3 %)	27 (84.6 %)

Table 2: Ranking of the new stations added to the base network under ~~eight~~ ten different sensitivity tests for the combined months of July and January. The tests are presented in the following order: surface grid height set at 60 m; surface grid height set at 75 m; trace of the posterior covariance used in the uncertainty metric; uncertainty of the night time observation errors is doubled; correlation structure is included in the prior covariance of the fluxes; spatial resolution is increased to 0.8°; spatial resolution is increased to 0.6°; ocean sources are assigned 10 % of max NPP variance; ocean sources are assigned 10 % of nearest terrestrial NPP variance; and GA is used for optimisation. The percentage cumulative reduction of uncertainty of the posterior fluxes relative to the base network is provided in brackets.

Rank	Ht 60 m	Ht 75 m	Trace	Night	Correl	Med Res	High Res	Ocean1	Ocean2	GA
1	18 (52.3)	18 (50.9)	18 (46.8)	18 (50.9)	24 (65.4)	18 (42.9)	18 (36.3)	18 (53.1)	18 (52.3)	27
2	29 (76.0)	29 (74.0)	29 (69.4)	29 (75.1)	11 (77.8)	29 (65.1)	28 (57.1)	29 (77.3)	29 (75.9)	7
3	11 (79.8)	11 (78.3)	11 (73.3)	11 (78.5)	28 (83.6)	11 (70.7)	11 (62.0)	11 (80.8)	11 (80.4)	29
4	22 (81.5)	24 (80.1)	22 (75.1)	22 (80.6)	31 (85.3)	30 (73.6)	30 (66.4)	22 (82.5)	22 (82.1)	18
5	27 (83.5)	27 (82.5)	27 (77.2)	27 (83.1)	27 (86.5)	27 (76.8)	24 (69.5)	27 (84.4)	27 (84.4)	11 (84.9)

Table 3: Table of network comparison statistics for the combined months of January and July. The sensitivity tests are presented in the same order as for Table 2.

Sensitivity Test	Uncertainty Reduction	Running Time (hh:mm)	Clustering Index
Standard	84.6 %	0:49	23.8
Ht 60 m	83.5 %	0:49	23.8
Ht 75 m	82.5 %	0:48	23.8
Trace	77.2 %	0:48	23.8
Night	83.1 %	0:48	23.8
Correl	86.5 %	1:13	17.4
Med Res	76.8 %	4:23	23.8
High Res	69.5 %	25:11	36.6
Ocean1	84.4 %	5:27	23.8
Ocean2	84.4 %	5:12	23.8
GA	84.9 %	32:01	17.4

Table 4: Table of dissimilarity indices for the optimal network solutions for the combined months of January and July. The sensitivity tests are presented in the same order as for Table 2.

Sensitivity Test	Standard	Ht 60 m	Ht 75 m	Trace	Night	Correl	Med Res	High Res	Ocean1	Ocean2	GA
Standard	0	0	469	0	0	1162	449	1121	0	0	1213
Ht 60 m	0	0	469	0	0	1162	449	1122	0	0	1213
Ht 75 m	469	469	0	469	469	761	380	720	469	469	1285
Trace	0	0	469	0	0	1162	449	1121	0	0	1213
Night	0	0	469	0	0	1162	449	1121	0	0	1213
Correl	1162	1162	761	1162	1162	0	1162	851	1162	1162	2046
Med Res	449	449	380	449	449	1162	0	741	449	449	1265
High Res	1121	1121	720	1121	1121	851	741	0	1121	1121	1693
Ocean1	0	0	469	0	0	1162	449	1121	0	0	1213
Ocean2	0	0	469	0	0	1162	449	1121	0	0	1213
GA	1213	1213	1285	1213	1213	2046	1265	1693	1213	1213	0

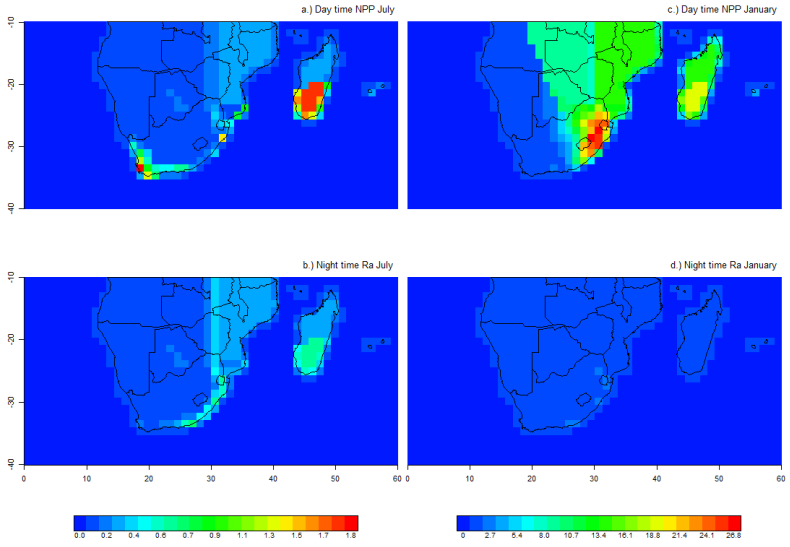

Fig. 1: The day time net primary productivity (NPP) and night time autotrophic respiration (Ra) data used as standard deviations of net ecosystem productivity (NEP) at the resolution of 1.2° expressed in gC/m^2/week for July (left) and January (right). Values for the standard deviation are capped at 28 gC/m^2/week. The maximum value (separately for day and night) is assigned to the non-South African land surface, or set at 28 gC/m^2/day if the maximum exceeds this value.

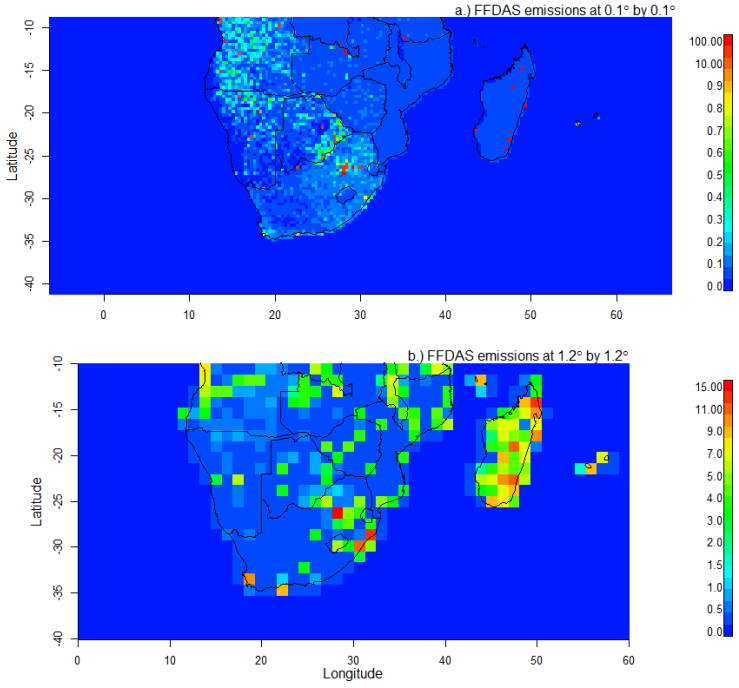

Fig. 2: The standard deviations of ten realisations (top) of the Fossil Fuel Data Assimilations System (FFADS) at the original 0.1° resolution in gC/m^2/week. The standard deviations of the aggregated fluxes (bottom) (1.2° resolution) showing significant smoothing of the fossil fuel fluxes over the lower resolution.

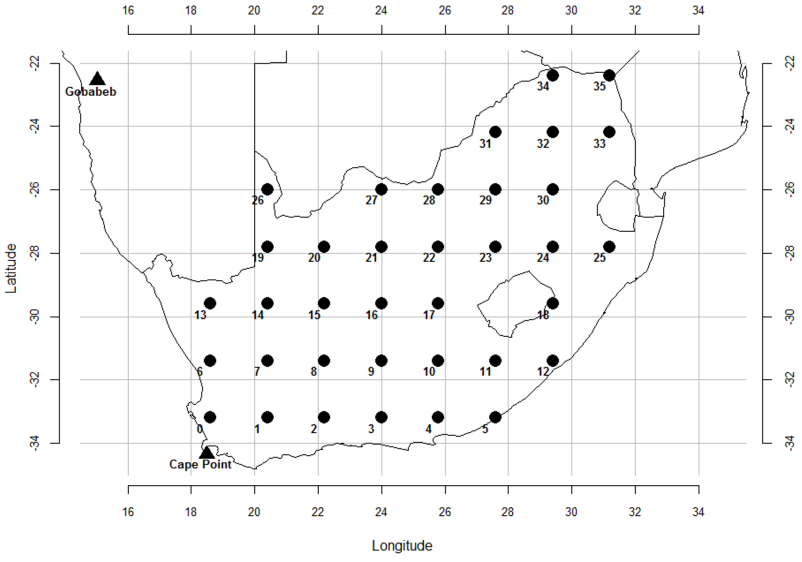

Fig. 3: The 36 potential locations of the new stations in the optimal network design. The locations were spaced on a regular grid over the surface of South Africa. The existing Cape Point and the Gobabeb GAW stations are marked by the triangles.

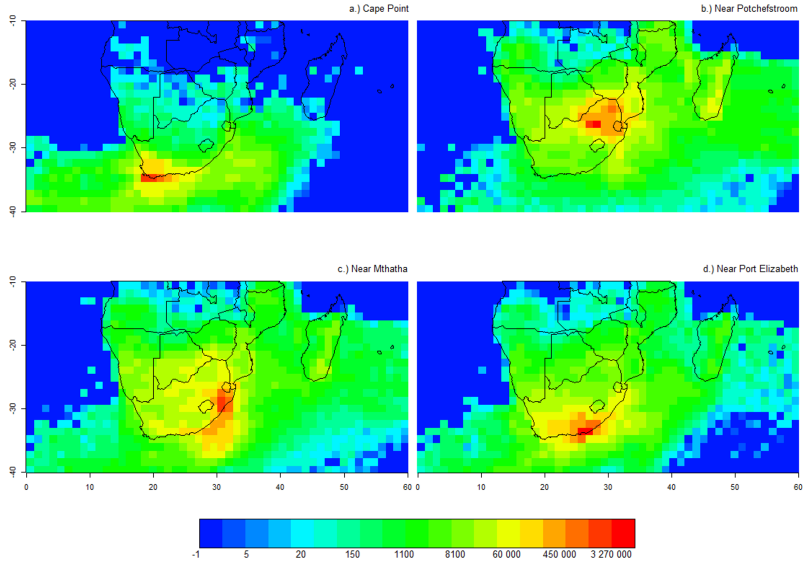

Fig. 4: The footprint of Cape Point, station 28 (top right), station 18 (bottom left), and station 4 (bottom right) relative to the surface grid cells at a resolution of 1.2° expressed as the count of particles over the month of January for each surface grid cell.

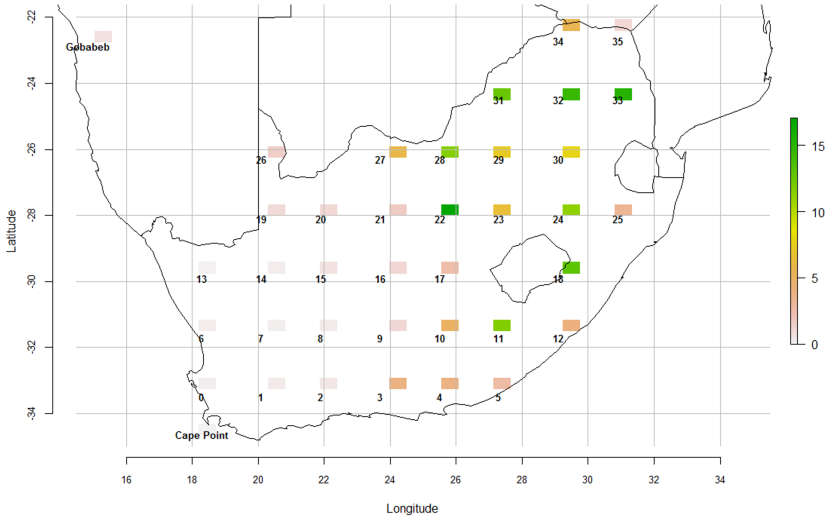

Fig. 5: Map of the aggregation error values (ppm) associated with each measurement station for the month of January.

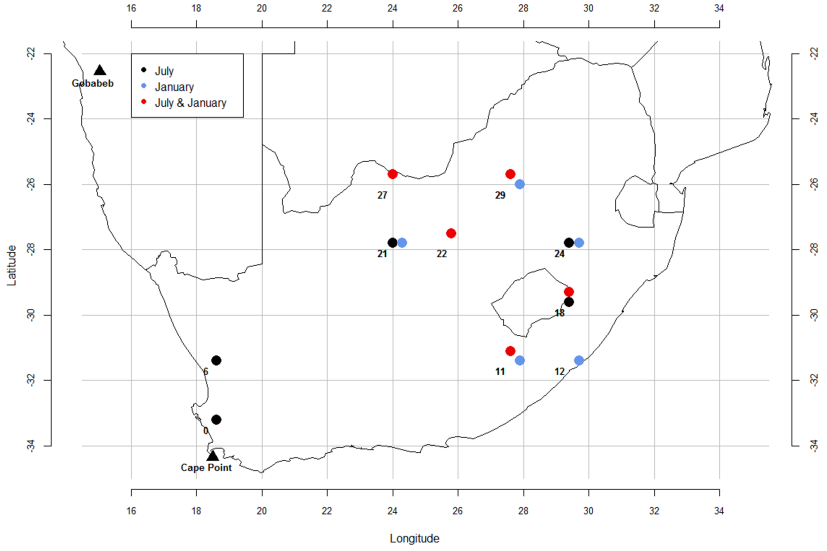

Fig. 6: Map of the optimal stations to add to the existing network to reduce the overall uncertainty of fluxes in South Africa for July, January, and the combined months of July and January. The standard network design conditions are: 50 m surface grid height, diagonal prior covariance, 2 ppm uncertainty in concentration observations, a 1.2° surface grid resolution, and the sum of the posterior covariance matrix elements used to calculate the uncertainty metric for the IO optimisation procedure.

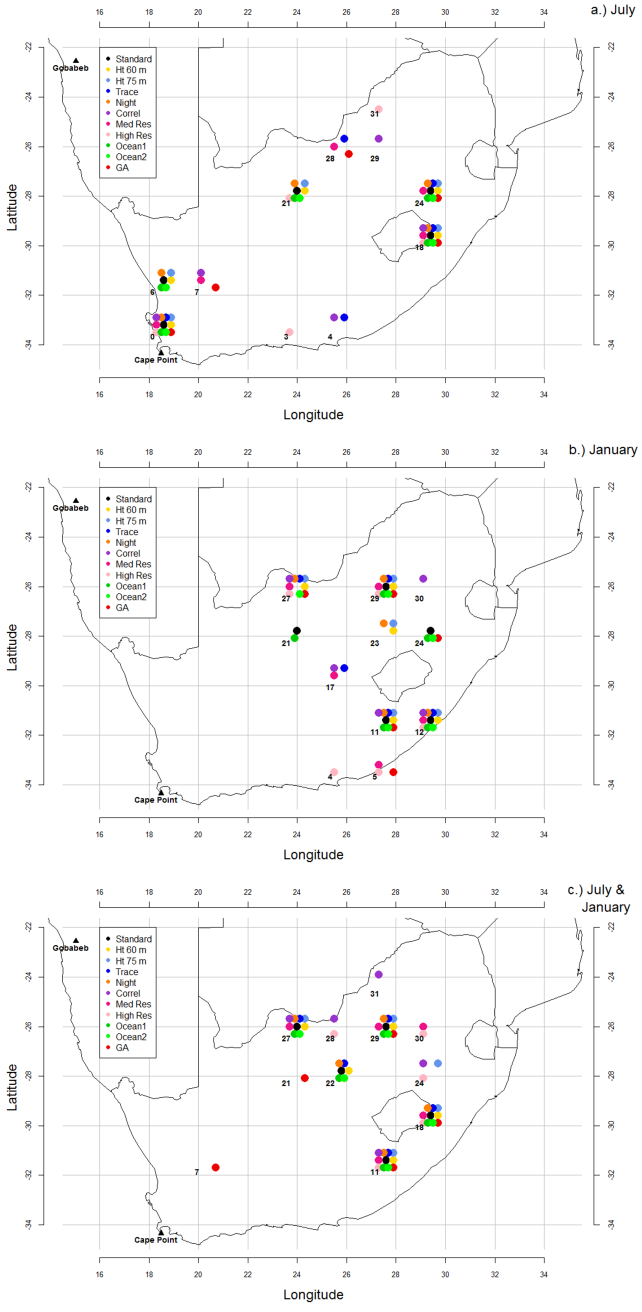

Fig. 7: Map of the optimal stations to add to the existing network to reduce the overall uncertainty of fluxes in South Africa under the eleven different sensitivity cases for July (top), January (middle), and the combined months of July and January (bottom). The cases include the standard case (Standard), surface grid height set at 60 m (Ht 60 m), surface grid height set at 75 m (Ht 75 m), use of the trace in the uncertainty metric (Trace), doubling of the night time observation error uncertainty (Night), addition of correlation between elements in the prior covariance matrix (Correl), spatial resolution set at 0.8° (Med Res), spatial resolution set at 0.6° (High Res), uncertainty in the ocean sources set at 10 % of the maximum land NPP (Ocean1), uncertainty in the ocean sources set at 10 % of the nearest land NPP (Ocean2), and use of the GA.

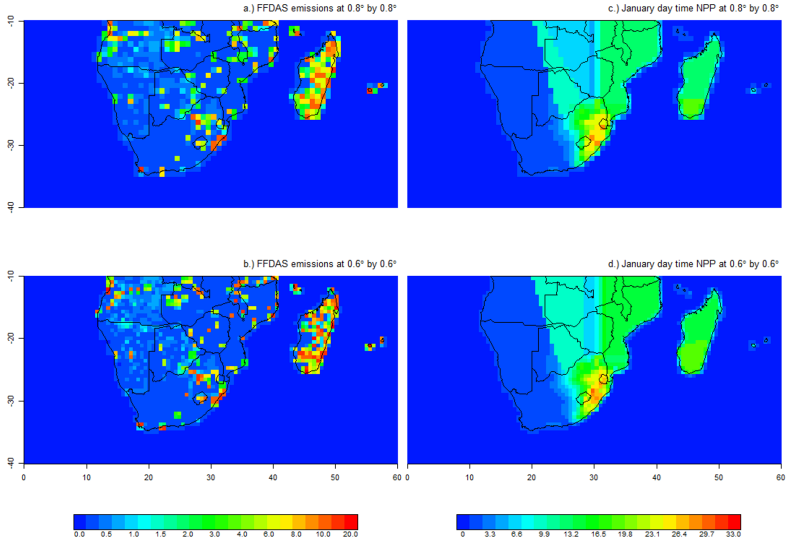

Fig. 8: The day time net primary productivity (NPP) data used as standard deviations of net ecosystem productivity (NEP) at the resolution of 0.8° expressed in gC/m^2/week for January (a), and at the resolution of 0.6° (b). The Fossil Fuel Data Assimilation System standard deviations aggregated over a resolution of 0.8°, also expressed in gC/m^2/week (c) and over a resolution of 0.8° (d).